



Does the presence of heterotrophic bacterium *Pseudomonas reactans* affect basaltic glass dissolution rates?

Gabrielle J. Stockmann^{a,b,*}, Liudmila S. Shirokova^{b,c}, Oleg S. Pokrovsky^b, Pascale Bénézech^b, Nicolas Bovet^d, Sigurdur R. Gislason^e, Eric H. Oelkers^{b,e}

^a Nordic Volcanological Center, Institute of Earth Sciences, University of Iceland, Sturlugata 7, 101 Reykjavík, Iceland

^b GET-Université de Toulouse-CNRS-IRD-OMP, 14 Avenue Edouard Belin, 31400 Toulouse, France

^c Institute of Ecological Problems of the North, 23 Nab. Severnoy Dviny, Russian Academy of Science, Arkhangelsk, Russia

^d Nano-Science Center, Department of Chemistry, University of Copenhagen, Universitetsparken 5, 2100 Copenhagen, Denmark

^e Institute of Earth Sciences, University of Iceland, Sturlugata 7, 101 Reykjavík, Iceland

ARTICLE INFO

Article history:

Received 23 July 2011

Received in revised form 11 December 2011

Accepted 12 December 2011

Available online 26 December 2011

Editor: J. Fein

Keywords:

Basaltic glass

Pseudomonas reactans

Mineral–bacteria interaction

Dissolution kinetics

Bacterial mixed-flow reactors

CO₂ sequestration

ABSTRACT

Far-from-equilibrium steady-state basaltic glass dissolution rates were measured using newly developed Bacterial Mixed-Flow Reactors (BMFR) at 25 °C. Experiments were performed in aqueous pH 4, 6, 8, and 10 buffer solutions with and without nutrients and in: 1) the absence of bacteria, 2) the presence of 0.1–0.4 g_{wet}/L dead *Pseudomonas reactans*, and 3) in the presence of 0.9–19.0 g_{wet}/L live *P. reactans* extracted from a deep subsurface oxygen-bearing basaltic aquifer. The BMFR allows steady-state rate measurements at constant concentrations of live or dead bacteria. Experiments ran for 30–60 days on a single basaltic glass powder, initially at bacteria- and nutrient-free conditions until Si steady-state glass dissolution was achieved. Then, in 2–4 steps, either live or dead *P. reactans* were added via nutrient-rich or nutrient-free inlet solutions, and the flux of Si and other mineral constituents from the basaltic glass were measured until a new chemical steady state was attained. Scanning Electron Microscope and X-ray Photoelectron Spectroscopic techniques verified the presence of live bacteria on the basaltic glass surfaces through biofilm formation, bacterial dissolution imprints, and enrichment of surface layers in C and N. The presence of either live or dead *P. reactans* lowers constant pH steady-state basaltic glass dissolution rates by no more than ~0.5 log units which is close to combined analytical and experimental uncertainties of the experiments. The presence of bacteria did not cause any significant modification in trace element release rates from dissolving basaltic glass within the uncertainty of the measurements. Experiments in nutrient-rich solutions yielded close to stoichiometric release of all major elements from basaltic glass at pH 6–8 likely as a result of organic ligand complexation with aqueous Al and Fe, which would otherwise form hydroxy-precipitates. As the results of this work suggest, at most, a small inhibiting effect of live or dead *P. reactans* on basaltic glass dissolution rates, geochemical modeling of mineral reactivity in basaltic aquifers likely does not require explicit provision for the presence of heterotrophic bacteria on basaltic glass reactivity.

© 2011 Elsevier B.V. All rights reserved.

1. Introduction

The role of bacteria on geochemical processes is receiving increasing attention as it has become apparent that bacteria can act as both a catalyst and an inhibitor of mineral precipitation and dissolution reactions (Ehrlich, 1981; Kalinowski et al., 2000; Ganor et al., 2009). Numerous laboratory and field studies have shown that bacteria can significantly affect alumino-silicate and metal oxide dissolution rates at Earth-surface conditions (Bennett and Casey, 1994; Vandevivere et al., 1994; Welch and Vandevivere, 1994; Grantham et al., 1997;

Hutchens et al., 2003; Edwards et al., 2004; Rogers and Bennett, 2004; Wu et al., 2007, 2008; Hutchens, 2009; Uroz et al., 2009; Hutchens et al., 2010). These observations may be due to several and sometimes competing effects including: a) fluid pH changes due to bacterial acid production or proton consumption (Wu et al., 2007, 2008), b) bacterial exometabolites and lysis production which may complex aqueous ions at the mineral surface and in the fluid phase, thereby changing the fluid saturation state with respect to the dissolving solid and/or secondary minerals, c) metal adsorption on cell walls (e.g. Fein et al., 1997) which together with aqueous metal complexation can alter multi-oxide mineral dissolution rates due to their dissolution mechanism (Gout et al., 1997; Oelkers and Schott, 1998; Schott et al., 2009), and d) biofilm formation, composed of exopolysaccharides (EPS), which could inhibit dissolution by blocking mineral surface–fluid interface (Welch and Vandevivere, 1994; Lee and Fein,

* corresponding author at: Nordic Volcanological Center, Institute of Earth Sciences, University of Iceland, Sturlugata 7, 101 Reykjavík, Iceland. Tel.: +354 857 4079; fax: +354 562 9767.

E-mail address: gjs3@hi.is (G.J. Stockmann).

2000; Buchardt et al., 2001; Hutchens et al., 2010). Certain soil Gram-positive bacteria have also been observed to promote silicate dissolution via acidic exopolysaccharide production (Belkanova et al., 1985, 1987; Malinovskaya et al., 1990). Due to the large number of bacterial influenced processes effecting mineral dissolution rates, bacteria may have distinct effects depending on its environment (Hutchens et al., 2006). In addition, certain bacteria have been observed to diversify their biofilm composition depending on the ions available to them (Liermann et al., 2000b).

To further our understanding of bacterial–surface interaction, this study reports basaltic glass dissolution rates in the presence and absence of heterotrophic bacteria. Generally, one would expect a different effect of bacteria on aluminosilicate reactivity compared to Al-free, Ca- and Mg-bearing “basic silicate” reactivity due to their different dissolution mechanisms (e.g., see Pokrovsky et al., 2009, 2010; Berner, 2010 for recent discussion). Basaltic glass represents an intermediate case between the aluminosilicate and “basic” silicates, because its dissolution requires removal of both Al, and Ca and Mg from the surface (c.f. Oelkers, 2001).

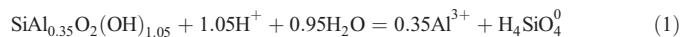
An additional motivation for this study is the potential for using basalts for carbon storage via mineral carbonatization (c.f. Oelkers and Schott, 2005; Oelkers et al., 2008a). This possibility is currently being tested at the Hellisheidi geothermal power plant in Iceland (Gislason et al., 2010). Heterotrophic aerobic bacteria, extracted from groundwater collected from well HK-31 at the Hellisheidi power plant (see Fig. 1), were used in this study of basaltic glass dissolution. Basaltic glass contains a large variety of major and trace elements allowing direct evaluation of the extent that weathering may be influenced by the solid’s nutritional potential (i.e. Bennett et al., 2001; Bailey et al., 2009).

Despite the fact that basaltic glass leaching in biotic soil and marine systems has been extensively investigated (Thorseth et al., 1992; Benedetti et al., 2003 and references therein), there are few laboratory

studies of basalt and basaltic glass interaction with bacteria available in the literature (Thorseth et al., 1995; Aouad et al., 2006; Wu et al., 2007). These studies, however, used batch reactors, in which the reactor fluid composition evolved continuously during the experiments. This approach prevents the rigorous determination of the dissolution rates required for the predictive modeling of water–rock interaction processes. The present work is aimed at overcoming these limitations by performing rate measurements in newly developed Bacterial Mixed-Flow Reactors (BMFR). BMFR reactors allow determination of water–rock reaction rates at constant bacterial concentrations and at steady-state conditions. The purpose of this paper is to present the results of basaltic glass dissolution rate measurements performed in these reactors and to use these results to better understand the role of bacteria on these rates.

2. Theoretical background

The standard state adopted in this study is that of unit activity of pure minerals and H₂O at any temperature and pressure. For aqueous species other than H₂O, the standard state is unit activity of species in a hypothetical 1.0 mol/kg solution referenced to infinite dilution at any temperature and pressure. Thermodynamic calculations reported in this study were performed using the PHREEQC 2.17 computer code (Parkhurst and Appelo, 1999) together with its llnl.dat and minteqv4.dat databases. The thermodynamic properties of hydrated leached basaltic glass with the composition, SiAl_{0.35}O₂(OH)_{1.05}, was added to the minteqv4 database. The equilibrium constant (K) for the leached glass dissolution reaction given by:



was calculated from the stoichiometric sum of the equilibrium constants of amorphous SiO₂ and amorphous Al(OH)₃ hydrolysis reactions (see

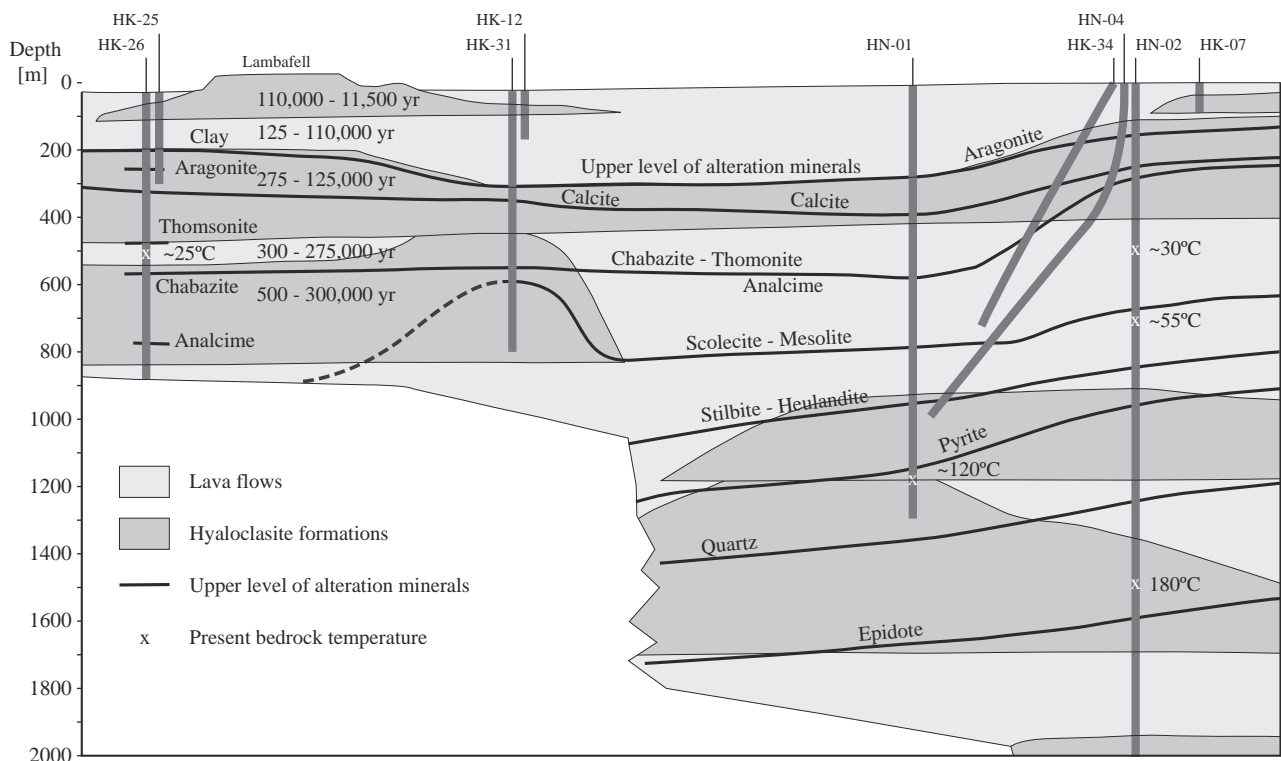


Fig. 1. Cross-section of the geological setting for the CO₂ injection at the Hellisheidi geothermal power plant in Iceland. The *Pseudomonas reactans* bacteria used for this study was extracted from water collected from well HK-31 at 400–800 m depth. Well HN-02 is the CO₂ injection well, HN-01 is the groundwater source, and HN-04, HK-34, HK-31 and HK-26 are the monitoring wells.

Modified from Alfredsson et al. (2008).

Bourcier et al., 1990; Wolff-Boenisch et al., 2004b and references therein). Log K for reaction (1) is calculated to be 1.07 and its corresponding ΔH_r to -22.47 kJ/mol at 25 °C.

Glass dissolution rates based on the release of the *i*th element ($r_{+,i}$, j) were calculated from:

$$r_{+,ij} = \frac{\Delta C_i \cdot fr}{\nu_i \cdot A_j \cdot m} \quad (2)$$

where ΔC_i stands for the concentration of the *i*th element in the outlet fluid minus its concentration in the inlet fluid, fr refers to the fluid flow rate, ν_i is a stoichiometric factor equal to the number of moles of the *i*th element in 1 mol of the glass (assumed to contain one Si atom), A_j designates the specific surface area of the basaltic glass, and m denotes the mass of glass used in the experiment. The index *j* refer to rates calculated either using the measured BET surface area, A_{BET} or the geometric surface area, A_{geo} .

Consistent with the dissolution mechanism and rate equations provided by Oelkers and Gislason (2001) and Gislason and Oelkers (2003), surface area normalized far-from-equilibrium basaltic glass dissolution rates can be quantified using:

$$r_{+,Si,j} = k \left(\frac{a_{H^+}^3}{a_{Al^{3+}}} \right)^{\frac{1}{2}} \quad (3)$$

where k denotes a rate constant, and j refer to rates normalized to either the BET surface area, A_{BET} or the geometric surface area, A_{geo} . Eq. (3) is based on the assumption that the rate-limiting step for basaltic glass dissolution is the liberation of partially detached Si tetrahedrons formed by the exchange of one adjacent Al with three aqueous protons (Oelkers, 2001; Oelkers and Gislason, 2001; Wolff-Boenisch et al., 2004b, 2006; Schott et al., 2009). According to Eq. (3), basaltic glass dissolution rates exhibit a U-shaped curve as a function of pH, which reaches a minimum around pH 6–7 at 25 °C. At high pH, the rates increase due to aqueous Al^{3+} complexation with hydroxide ions forming $Al(OH)_4^-$. Similar U-shaped dissolution rate versus pH curves are found for other aluminum-containing silicates, i.e. feldspars (Oelkers and Schott, 1998) and muscovite (Oelkers et al., 2008b). Any complexing of aqueous Al^{3+} at low pH with anions like F^- and SO_4^{2-} , or organic molecules leads to increased basaltic glass dissolution rates (Oelkers and Gislason, 2001; Wolff-Boenisch et al., 2004a, 2011; Flaathen et al., 2010), whereas at high pH aqueous Al–OH complexing is strong and the rates are relatively unaffected by other complexing ions (Wolff-Boenisch et al., 2004a; Flaathen et al., 2010; Wolff-Boenisch et al., 2011).

The elements released by basaltic glass dissolution in the presence of bacteria and exometabolites can a) remain free aqueous ions, b) complex with cell exometabolites, c) adsorb on the bacteria surface, d) be consumed and assimilated into bacteria cells and/or e) be sequestered by secondary minerals (Neaman et al., 2005a,b, 2006; Shirokova et al., 2012). Bacterial surfaces contain large quantities of functional groups including carboxyl, hydroxyl, and phosphoryl groups (Fein et al., 1997), and exometabolites comprised of long organic sugar molecules, together with pieces of lysed and dead bacteria cells. Both surface complexes and exometabolites could affect mineral dissolution, through complexing with the aqueous Al^{3+} and divalent cations, primarily Ca^{2+} , Mg^{2+} and Fe^{2+} . Complexing aqueous Al^{3+} could lead to increased dissolution rates of basaltic glass at low pH as described by Wolff-Boenisch et al. (2004a) and Flaathen et al. (2010), whereas bacterial surface adsorption or intracellular consumption of divalent cations would decrease element availability for secondary mineral precipitation. Surface passivation via binuclear or multinuclear complex formation is another possible rate inhibition mechanism of microorganisms and their exometabolites and lysis products.

3. Material and methods

3.1. Basaltic glass

The basaltic glass used in this study was collected from the Stapafell Mountain in Southwest Iceland and is the same material as was previously described by Oelkers and Gislason (2001), Gislason and Oelkers (2003), and Stockmann et al. (2011). A size fraction of 45–125 μm basaltic glass was used for all experiments performed in this study. The grinding, sieving, and cleaning procedures of this glass powder were described in detail by Stockmann et al. (2011). The chemical composition of the basaltic glass, as determined by X-ray Fluorescence analysis, is listed in Table 1 and is consistent with the formula: $Si_{1.000} Al_{0.350} Fe_{0.187} Mn_{0.003} Mg_{0.292} Ca_{0.263} Na_{0.076} K_{0.007} Ti_{0.024} P_{0.004} O_{3.371}$. The Fe^{2+}/Fe^{3+} -ratio of this glass was not determined, but Oelkers and Gislason (2001) reported iron in Stapafell basaltic glass to be predominantly Fe^{2+} . Trace element analysis is included in Table 1 and selected trace elements were chosen to test the effect of bacteria uptake and absorption in this study.

The specific surface area, A_{BET} , of the cleaned basaltic glass powder was determined to 5878 ± 400 cm^2/g by the multi-point krypton adsorption BET method, and the geometric surface area, A_{geo} , was calculated to 251 cm^2/g (Stockmann et al., 2011). Dividing the BET surface area by the geometric yields a roughness factor of 23. Surface roughness and fine-scale porosity within the glass are the likely reasons for the higher BET surface area compared to the geometric surface area. Dissolution rates of basaltic glass based on both BET and geometric surface areas are reported in this study. However, BET dissolution rates are shown in figures to be consistent with previous reports of abiotic basaltic glass dissolution (Oelkers and Gislason, 2001; Gislason and Oelkers, 2003; Stockmann et al., 2011). Additional BET measurements were performed on the basaltic glass at the end of selected experiments to assess if the dissolution in the presence of bacteria had dramatically affected surface areas.

3.2. Bacterial culture

Bacteria were extracted from groundwater collected from well HK-31 at the Hellisheidi power plant from 400 to 800 m depth (see Fig. 1). Water chemistry data from HK-31 at the time of sampling is provided in Table 2. Heterotrophic aerobic Gram-negative strain of *Pseudomonas reactans* (called HK 31.3), as identified by DNA extracting (UltraClean® Microbial DNA Isolation Kit MO BIO) and 16S rRNA gene amplifying (Shirokova et al., 2012), was separated and purified

Table 1
Chemical composition of basaltic glass from the Stapafell Mountain, SW Iceland. Results of X-ray fluorescence analysis (XRF).

Major elements ^{a,b}	Weight %	Trace elements							
		ppm		ppm		ppm		ppm	
SiO ₂	48.55	Ag	0.031	Hf	1.89	Sr	201	Cs	<0.1
Al ₂ O ₃	14.43	As	0.126	Hg	0.004	Ta	0.717	Pr	3.42
CaO	11.94	Au	0.005	Li	4.27	Te	0.016	Nd	15.1
Fe ₂ O ₃	12.08	B	1.06	Mo	0.901	Th	0.944	Sm	3.74
FeO	–	Ba	79.6	Nb	15.5	Tl	0.011	Eu	1.31
K ₂ O	0.274	Be	0.704	Ni	153	U	0.248	Gd	4.26
MgO	9.51	Bi	0.008	Pb	0.841	V	296	Tb	0.653
MnO	0.192	Cd	0.147	Rb	6.84	W	0.253	Dy	4.17
Na ₂ O	1.91	Co	51.9	Re	0.001	Y	21.6	Ho	0.817
P ₂ O ₅	0.199	Cr	646	S	326	Zn	162	Er	2.51
TiO ₂	1.570	Cu	136.2	Sb	0.054	Zr	95.3	Tm	0.345
		Ga	15.5	Sc	40.4	La	11.9	Yb	2.15
Total	100.00	Ge	1.90	Sn	1.92	Ce	26.3	Lu	0.331

^a Major elements were re-analyzed at the University of Edinburgh, 2011 and thus differs slightly from values in Stockmann et al. (2011).

^b Fe₂O₃ represents total Fe in the glass. Oelkers and Gislason (2001) determined Fe to be predominantly Fe^{2+} in Stapafell basaltic glass.

Table 2

Water chemistry data for well HK-31 at Hellisheidi, Iceland.

source: Shirokova et al. (2012) except for O₂ which was obtained by H.A. Alfredsson (personal comm., 2011).

pH _{exit}	9.44
T _{exit}	18.2 °C
Na	46 mg/l
Si	16 mg/l
Ca	3.6 mg/l
Mg	0.6 mg/l
Al	50 µg/l
Fe	8 µg/l
O ₂	0.081 mmol/L
DOC	0.44 ppm

using agar plate technique and cultured under laboratory conditions in nutrient broth-rich (NB) media. *P. reactans* is a common rod-shaped groundwater and soil bacteria averaging 2 µm in size; it has already reported to occur in underground Siberian water repositories (Nazina et al., 2006, 2010). A further description of *P. reactans* is provided by Shirokova et al. (2012). Freshly-grown bacterial cultures having the identical age, physiological, and initial nutritional status were used in all experiments.

Dead (heat-killed) cells were produced via autoclaving a freshly grown bacterial biomass for 30 min at 130 °C, followed by thorough rinsing in sterile 0.1 M NaCl. Although the heat-killing procedure can significantly modify the cell surface structure, it still remains a widely used method for producing biological control material (e.g. Ngwenya, 2007; Martinez et al., 2008; Pokrovsky et al., 2008; Kenward et al., 2009; Martinez et al., 2010). Scanning electron and optical microscopic examination showed that heat-killed cells maintained their integrity and shape after heat treatment. Inactivated cells were produced using 0.01 M sodium azide (NaN₃) during selected experiments. The use of NaN₃ as metabolic inhibitor for heterotrophic bacteria is well established in the literature (i.e., Urrutia Mera et al., 1992; Johnson et al., 2007).

Active bacteria number counts (colony forming-units, CFU/mL) were performed using Petri dish inoculation on nutrient agar (0.1, 0.2, and 0.5 mL of sampled solution in three replicates) in a laminar hood box. Inoculation of blanks was routinely performed to assure the absence of external contamination. The biomass of live bacteria suspensions was also quantified by measuring wet (after it was centrifuged 15 min at 10,000 rpm) and freeze-dried weight in duplicates. The conversion ratio wet/freeze-dried weight of the studied microorganisms is equal to 8.4 ± 0.5 . The conversion factor of optical density (600 nm, 10 mm path) and wet biomass (g_{wet}/L) to the cell number (CFU/mL) was equal to $(5 \pm 1) \times 10^8$ and $(8.0 \pm 1.5) \times 10^7$, respectively as determined by triplicate measurements. Live biomass concentration during BMFR experiments ranged from 0.9 to 19 g_{wet}/L. Before the preparation of the inlet fluid for BMFR experiments, cells were rinsed twice in either the appropriate fresh culture media or a sterile 0.1 M NaCl solution using centrifugation with ~500 mL of solution for 1 g of wet biomass, to remove adsorbed metals and cell exudates from the surface.

3.3. Dissolution rate experiments in Bacterial Mixed-Flow Reactors (BMFR)

Steady-state basaltic glass dissolution rates were obtained at distinct fluid compositions and pH using a Bacterial Mixed-Flow Reactor (BMFR) system; the design of this system is shown in Fig. 2. This system consists of a 40 ml mixed-flow reaction vessel immersed in a water bath held at a constant temperature of 25.0 ± 0.5 °C. This reactor is fitted with 10 or 20 µm poresize Magna Millipore Nylon outlet filters to allow bacteria to pass while retaining the 45–125 µm glass powder in the reactor. This reactor system thus maintained a constant biomass concentration in the reactor, equal to that of the inlet fluid. The input fluids were kept in 1 L polypropylene bottles closed with Biosilico® ventilated caps. These fluids were stirred continuously during the experiments and were changed typically each 7 days. This allowed maintenance of a constant and stable stationary phase bacterial culture in the bacteria-bearing inlet fluids. Bacteria concentration was verified by periodic sampling of inlet and outlet fluids for cell optical density (total biomass) and live cell numbers (via agar plate counting). Prior to each

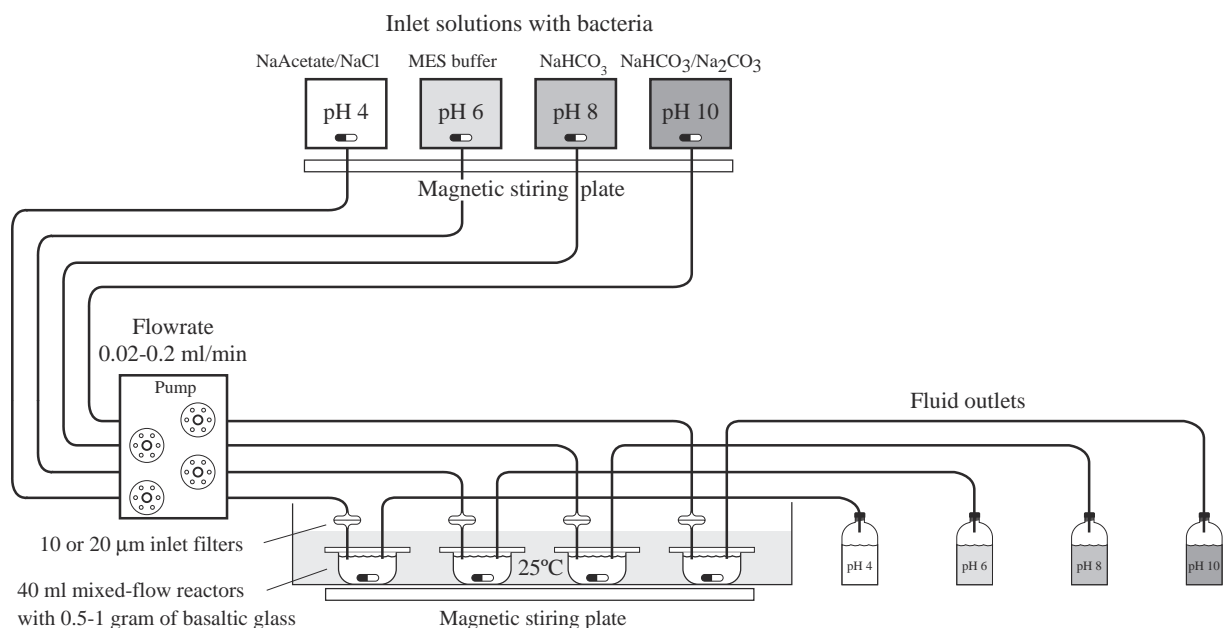


Fig. 2. Reactor system used for the experiments performed in this study. Inlet solutions containing bacteria were continuously stirred to keep solutions homogenous. Outlet solutions passed through 10 or 20 µm filters, which allow bacteria to pass while retaining the basaltic glass powder.

Table 3a

Summary of experimental results at steady state for all the basaltic glass dissolution experiments performed in this study. All experiments were performed at 25 °C.

Exp. ^a	m _{BC} (g)	S _{BET} (m ²)	Fr (g/min)	Duration (days)	pH _{in}	pH _{out}	Bact _{in} ^b (mg _{wet} /L)	Bact. status ^c	Nutr _{in} (%)	Bact _{out} ^b (CFU/mL)	DOC _{out} (mg/L)	[Si] ^d (μmol/kg)	[Al] ^d (μmol/kg)	[Ca] ^d (μmol/kg)	[Mg] ^d (μmol/kg)	[Fe] ^d (μmol/kg)
4-1	1.00	0.59	0.03	15	4.07	4.33	0		0			36.57	15.64	22.95	26.75	10.8
4-2	0.97	0.57	0.02	14	4.58	4.63	100	Dead	0			17.19	1.85	b.d.	3.99	0.61
4-3	0.97	0.57	0.03	11	4.28	4.58	430	Dead	0			10.79	1.38	5.30	2.80	0.43
4-4 ^e	0.89	0.53	0.02	22	4.18	7.44	700	Live	0	1.0E + 07		11.14	0.39	2.17	4.70	0.22
6-1	0.52	0.30	0.33	4	5.86	5.92	0		0			0.60				
6-2	0.52	0.30	0.21	3	5.81	5.98	0		0			0.84				
6-3	0.52	0.30	0.21	3	6.22	6.38	0		1			0.58				
6-4	0.52	0.30	0.21	6	6.33	6.44	0		10			1.30				
6-5	0.94	0.55	0.23	7	6.05	6.04	0		0			1.98	0.06		0.51	
6-6	0.94	0.55	0.22	9	6.12	6.15	11.8	Dead	0			0.63	0.06		0.21	
6-7	0.94	0.55	0.22	4	6.12	6.17	100	Dead	0			0.62	0.11			
6-8	0.94	0.55	0.22	2	6.16	6.19	198	Dead	0			0.68				
6-9	0.94	0.55	0.22	15	6.40	6.35	368	Dead	0			b.d.	0.21		0.87	
6-10	1.05	0.62	0.02	21	6.10	6.19	0		0			13.10	0.14	5.09	3.29	0.04
6-11	1.00	0.59	0.02	26	6.23	6.32	200	Dead	0			b.d.	b.d.	b.d.	0.92	0.004
6-12	1.00	0.59	0.02	11	6.10	6.24	430	Dead	0			6.72	0.04	6.71	1.46	b.d.
6-13 ^e	0.94	0.55	0.02	22	6.08	6.02	700	Live	0	2.8E + 07		4.45	0.58	b.d.	3.75	0.15
E5-1	0.98	0.57	0.02	8	n.m.	6.59	0		0			23.00	0.67	7.29	7.24	0.93
E5-2	0.98	0.57	0.02	7	n.m.	6.22	870	Live	0	6.0E + 07		15.90	0.29	11.4	2.80	0.34
E5-3	0.98	0.57	0.02	12	n.m.	7.15	6500	Live	0			8.51	0.52	9.63	2.80	0.70
E3-1	1.03	0.61	0.02	13	n.m.	7.43	0		10			18.16	6.38	7.56	11.44	2.22
E3-2	1.03	0.61	0.02	12	n.m.	7.78	8900	Live	10	9.0E + 08		18.65	3.45	5.89	5.06	2.17
E3-3	1.03	0.61	0.02	6	n.m.	7.62	12,000	Live	10			19.19	1.96	6.69	6.05	2.20
8-1	0.50	0.3	0.42	4	7.92	7.92	0		0			1.23				
8-2	0.50	0.3	0.28	3	7.94	7.91	0		0			1.18				
8-3	0.50	0.3	0.28	3	7.83	7.34	0		1			0.79				
8-4	0.50	0.3	0.28	6	7.89	7.67	0		10			0.46				
8-5	0.96	0.56	0.26	7	8.55	8.37	0		0			3.41	1.19		0.81	
8-6	0.96	0.56	0.26	9	8.46	8.24	12	Dead	0			2.41	0.78		0.49	
8-7	0.96	0.56	0.26	4	8.33	8.04	70	Dead	0			1.70	0.40			
8-8	0.96	0.56	0.26	2	8.55	8.04	195	Dead	0							
8-9	0.96	0.56	0.25	13	8.10	8.01	368	Dead	0			0.59	0.26		0.83	
8-10	1.01	0.59	0.03	21	8.55	8.89	0		0			28.32	10.53	2.32	5.54	0.89
8-11	0.99	0.58	0.03	26	8.57	8.63	200	Dead	0			11.57	2.53	0.56	3.13	0.05
8-12	0.99	0.58	0.02	11	8.36	8.61	430	Dead	0			34.43	1.10	12.5	5.06	b.d.
8-13 ^e	0.98	0.58	0.02	22	8.53	7.93	700	Live	0	2.5E + 08	18.0	15.49	3.37	4.05	8.83	1.56
E6-1	1.06	0.63	0.02	8	n.m.	8.99	0.0		0			21.41	6.82	3.77	7.49	0.48
E6-2	1.06	0.63	0.02	7	n.m.	8.74	870	Live	0	8.3E + 07	8.4	18.69	4.34	9.31	5.80	0.70
E6-3	1.06	0.63	0.02	12	n.m.	8.48	6500	Live	0		33.3	18.37	2.47	4.84	7.45	0.20
E4-1	1.16	0.68	0.02	13	n.m.	8.02	0.0		10			20.54	3.26	6.54	5.72	1.83
E4-2	1.16	0.68	0.02	12	n.m.	8.06	8900	Live	10			17.87	2.15	4.37	6.01	1.34
E4-3	1.16	0.68	0.02	6	n.m.	7.90	19,000	Live	10			18.65	2.47	4.69	13.04	2.61
10-1	0.99	0.58	0.03	15	10.05	9.99	0		0			117.89	31.47	8.51	18.2	1.07
10-2	0.93	0.55	0.03	14	10.02	9.83	100	Dead	0			100.99	23.31	13.65	14.92	1.04
10-3	0.93	0.55	0.03	11	9.94	9.01	430	Dead	0			68.81	11.60	11.88	8.38	1.40
10-4 ^e	0.80	0.47	0.02	22	10.11	8.35	700	Live	0	3.3E + 07	17.5	14.99	6.31	5.10	68.35	0.39

n.m.: not measured.

b.d.: below detection limit.

^a Each experimental series is denoted by the solid horizontal lines drawn in the table.^b Concentration of *Pseudomonas reactans* in inlet (Bact_{in}) and outlet (Bact_{out}) solution measured in mg_{wet}/L and colony-forming units (CFU/mL), respectively.^c Dead *Pseudomonas reactans* (dead) plus NaN₃ or live *Pseudomonas reactans* (live) ± nutrient broth was added to the inlet solution.^d Concentration of element determined from its concentration in the outlet fluid minus its concentration in the inlet fluid.^e The amount of Si, Al, Ca, Mg and Fe in the inlet solutions is estimated from the concentration of these ions in experiments with the same inlet electrolyte and bacteria concentration.

experiment, all reactor system parts including tubing were sterilized at 130 °C for 30 min and rinsed with sterile MilliQ water.

The experiments conducted within in this study can be divided into three categories 1) bacteria- and nutrient-free, 2) dead bacteria in nutrient-free media, and 3) live bacteria. Live bacteria experiments can further be subdivided into two categories: 3a) nutrients added and 3b) no nutrients added. Experiments were performed in series. At the beginning of each series 0.5–1 g of fresh basaltic glass powder was added to the reactor system. A sterile bacteria-free fluid was injected into the reactor at a constant flow rate until a steady-state

outlet fluid composition was attained. This provided a reference point, to compare results with subsequent bacteria-bearing dissolution experiments. Once steady state was attained, live or dead bacteria ± nutrients or sodium azide (NaN₃) were added to this inlet solution. Sodium azide was added to the inlet fluids containing dead bacteria to avoid any possible external contamination and bacterial growth during the experiment. Additional live or dead bacteria were added to the inlet fluid after a second steady-state element release rate was attained. This step was repeated until the experimental series was stopped. To assess the effect of nutrients on rates, a 1:10 diluted Aldrich nutrient

Table 3bSteady-state dissolution rates, $\log(r_{+,i,j}/(\text{mol}/\text{cm}^2/\text{s}))$ for basaltic glass at 25 °C determined in the present study.

Exp. a	pH _{out} (25 °C)	Bact _{in} ^b (mg/L)	Bact. status ^c	Nutr _{in} (%)	A* ^{d,e} (kJ/mol)	Log $r_{+,Si,BET}$	Log $r_{+,Si,geo}$	Log $r_{+,Al,BET}$	Log $r_{+,Al,geo}$	Log $r_{+,Ca,BET}$	Log $r_{+,Ca,geo}$	Log $r_{+,Mg,BET}$	Log $r_{+,Mg,geo}$	Log $r_{+,Fe,BET}$	Log $r_{+,Fe,geo}$
4-1	4.33	0		0	18.15	-14.57	-13.20	-14.48	-13.11	-14.19	-12.82	-14.17	-12.80	-14.37	-13.00
4-2	4.63	100	Dead	0		-14.94	-13.57	-15.45	-14.08			-15.04	-13.67	-15.66	-14.29
4-3	4.58	430	Dead	0		-15.10	-13.73	-15.54	-14.17	-14.83	-13.46	-15.16	-13.79	-15.78	-14.41
4-4	7.44	700	Live	0		-15.11	-13.74	-16.11	-14.74	-15.24	-13.87	-14.95	-13.58	-16.09	-14.72
6-1	5.92	0		0	23.46 ^f	-14.96	-13.59								
6-2	5.98	0		0	22.20 ^f	-15.01	-13.64								
6-3	6.38	0		1		-15.18	-13.81								
6-4	6.44	0		10		-14.83	-13.46								
6-5	6.04	0		0	21.40 ^g	-14.87	-13.50	-15.93	-14.56			-14.93	-13.56		
6-6	6.15	11.8	Dead	0		-15.37	-14.00	-15.94	-14.57			-15.32	-13.95		
6-7	6.17	100	Dead	0		-15.38	-14.01	-15.68	-14.31						
6-8	6.19	198	Dead	0		-15.35	-13.98								
6-9	6.35	368	Dead	0				-15.40	-14.03			-14.71	-13.34		
6-10	6.19	0		0	15.81 ^g	-15.09	-13.72	-16.59	-15.22	-14.92	-13.55	-15.16	-13.79	-16.88	-15.51
6-11	6.32	200	Dead	0								-15.75	-14.38	-17.92	-16.55
6-12	6.24	430	Dead	0		-15.47	-14.10	-17.23	-15.87	-14.89	-13.52	-15.59	-14.22		
6-13	6.02	700	Live	0		-15.57	-14.20	-16.00	-14.63			-15.11	-13.74	-16.31	-14.94
E5-1	6.59	0		0	13.18 ^g	-14.87	-13.50	-15.95	-14.58	-14.79	-13.42	-14.84	-13.47	-15.54	-14.17
E5-2	6.22	870	Live	0		-15.06	-13.69	-16.34	-14.97	-14.62	-13.25	-15.28	-13.91	-16.00	-14.63
E5-3	7.15	6500	Live	0		-15.31	-13.94	-16.06	-14.69	-14.67	-13.30	-15.25	-13.88	-15.66	-14.29
E3-1	7.43	0		10		-15.00	-13.63	-15.00	-13.63	-14.80	-13.43	-14.67	-13.30	-15.19	-13.82
E3-2	7.78	8900	Live	10		-14.99	-13.62	-15.27	-13.90	-14.91	-13.54	-15.02	-13.65	-15.20	-13.83
E3-3	7.62	12,000	Live	10		-15.00	-13.63	-15.53	-14.17	-14.88	-13.51	-14.97	-13.60	-15.21	-13.84
8-1	7.92	0		0	23.17 ^f	-14.53	-13.17								
8-2	7.91	0		0	23.34 ^f	-14.73	-13.36								
8-3	7.34	0		1		-14.90	-13.53								
8-4	7.67	0		10		-15.13	-13.76								
8-5	8.37	0		0	20.72	-14.58	-13.21	-14.58	-13.21			-14.67	-13.30		
8-6	8.24	12	Dead	0		-14.73	-13.36	-14.76	-13.40			-14.89	-13.52		
8-7	8.04	70	Dead	0		-14.89	-13.52	-15.06	-13.69						
8-8	8.04	195	Dead	0											
8-9	8.01	368	Dead	0		-15.36	-13.99	-15.26	-13.89			-14.67	-13.30		
8-10	8.89	0		0	16.50	-14.70	-13.33	-14.68	-13.31	-15.21	-13.84	-14.88	-13.51	-15.48	-14.11
8-11	8.63	200	Dead	0		-15.08	-13.71	-15.29	-13.92	-15.82	-14.45	-15.12	-13.75	-16.72	-15.35
8-12	8.61	430	Dead	0		-14.73	-13.36	-15.77	-14.40	-14.59	-13.22	-15.03	-13.66		
8-13	7.93	700	Live	0		-14.99	-13.62	-15.20	-13.83	-14.99	-13.62	-14.70	-13.33	-15.26	-13.89
E6-1	8.99	0.0		0	16.15	-14.92	-13.55	-14.96	-13.59	-15.10	-13.73	-14.84	-13.47	-15.84	-14.47
E6-2	8.74	870	Live	0		-14.96	-13.59	-15.14	-13.77	-14.68	-13.31	-14.93	-13.56	-15.66	-14.29
E6-3	8.48	6500	Live	0		-14.95	-13.58	-15.36	-13.99	-14.95	-13.58	-14.81	-13.44	-16.18	-14.81
E4-1	8.02	0.0		10		-15.00	-13.63	-15.34	-13.97	-14.91	-13.54	-15.02	-13.65	-15.32	-13.95
E4-2	8.06	8900	Live	10		-15.08	-13.71	-15.54	-14.17	-15.11	-13.74	-15.02	-13.65	-15.48	-14.11
E4-3	7.90	19,000	Live	10		-15.08	-13.71	-15.51	-14.14	-15.10	-13.73	-14.70	-13.34	-15.21	-13.84
10-1	9.99	0		0	16.44	-14.06	-12.69	-14.18	-12.81	-14.62	-13.25	-14.33	-12.96	-15.37	-14.00
10-2	9.83	100	Dead	0		-14.11	-12.75	-14.30	-12.93	-14.40	-13.03	-14.41	-13.04	-15.37	-14.00
10-3	9.01	430	Dead	0		-14.26	-12.89	-14.58	-13.21	-14.45	-13.08	-14.64	-13.27	-15.23	-13.86
10-4	8.35	700	Live	0		-14.90	-13.53	-14.82	-13.45	-14.78	-13.42	-13.70	-12.33	-15.75	-14.38

^a Each experimental series is denoted by the solid horizontal lines drawn in the table.^b Concentration of *Pseudomonas reactans* in inlet (Bact_{in}) solution measured in mg_{wet}/L.^c Either dead *Pseudomonas reactans* plus NaNO₃ or live *Pseudomonas reactans* was added to the inlet solution.^d Chemical affinity of hydrated basaltic glass layer.^e Calculated by PHREEQC modeling version 2.17.^f Calculated with hypothetical stoichiometric release of [Al].^g Modeled with PHREEQC assuming same inlet solution as in experiments 6-1 to 6-4.

broth, comprised of 0.1 g/L glucose, 1.5 g/L peptone, 0.6 g/L NaCl, and 0.3 g/L yeast extract, was added to selected live bacteria experiments. These experiments were compared to live bacteria experiments performed with no added nutrients. During 4 of the experimental series (following experiments 4–3, 6–12, 8–12, and 10–3) less than 10% of the basaltic glass was removed for SEM analysis. In all other cases, all of the original basaltic glass remained in the reactor until the experimental series was completed.

The chemical compositions of each individual inlet solution used for the experiments in this study are listed in Appendix 1 along with its ionic strength and pH at 25 °C. Inlet fluids were comprised of MilliQ

water and analytical grade chemicals including NH₄Cl, NH₄OH, Na-acetate, C₆H₁₃NO₄S ('MES' buffer), NaHCO₃, Na₂CO₃, NaCl (99.5% pure), HCl, and NaOH. Experimental series were performed using four distinct inlet pH buffers: 4, 6, 8, and 10, comprised of a 0.01 M Na acetate–NaCl–HCl solution, a 0.001 M or 0.01 M MES solution, a 0.01 M NaHCO₃ solution, and a 0.004 M NaHCO₃ + 0.003 M Na₂CO₃ solution, respectively. The ionic strength was ~0.01 mol/kg for the pH 4, 8, and 10 inlet fluids and 0.001 or 0.01 mol/kg for the pH 6 inlet fluids. Inlet fluid pH generally remained stable within ±0.1 units throughout each experimental series. Outlet fluid pH varied within ±0.3 units, except for the live bacteria experiments performed at pH 4 and 10,

where pH changed by as much as ± 3.0 units from the initial to the steady-state value. All outlet fluid samples were filtered through $0.45\ \mu\text{m}$ Millipore acetate cellulose filters and acidified with ultrapure 2% HNO_3 before chemical analysis. The exception was samples collected for dissolved organic carbon determination, which were filtered and stored at $4\ ^\circ\text{C}$ before the analysis. Inlet fluids were routinely analyzed at the beginning, in the middle, and at the end of each experiment and were filtered and processed using exactly the same protocol as the outlet fluids. All chemistry data for the outlet fluids at steady-state are provided in Tables 3a and 3b.

To assess possible adsorption of released aqueous metals to biomass surfaces additional non-filtered outlet fluid samples were collected, and 0.01 M EDTA was added to these unfiltered samples. After 10 min the biomass was separated using centrifugation. The amount of Mg, Ca, and Al released to the fluid after this EDTA treatment was considered to be reversibly adsorbed on the surface (e.g., Knauer et al., 1997; Le Faucher et al., 2005). This amount never exceeded 10% of total dissolved ($<0.45\ \mu\text{m}$) filtered concentration of each metal and therefore was not considered in the mass balance calculations presented below.

Mechanical steady state was achieved in the BMFR after 24 h of reaction. Chemical steady state was assumed when measured Mg, Ca, Al, Si, and trace metal concentrations varied by less than 5% for concentrations of $\geq 5\ \mu\text{M}$ but 15% for concentrations of $<5\ \mu\text{M}$ in 4 to 5 samples collected at least 24 h apart. Measured steady-state Mg, Ca, Al, Si, and trace metal concentrations and fluid flow rates (reproducibility of $\pm 10\%$) were used for calculating dissolution rates. The largest uncertainty on reported rates generated in this study stem from the ΔC_i values in Eq. (2). As the analytical uncertainty was 5–10% and

the experimental reproducibility was 10–20% the overall uncertainty on $\log R_{\text{Me}}$, and $\log R_{\text{Si}}$ values reported in this study range from 0.1 to 0.2 units.

3.4. Batch experiments performed to assess live bacteria interaction with mineral-free solutions in the presence of mineral constituents

These experiments were designed to quantify the amount of basaltic glass constituents (Mg, Ca, Al, Si, metals) retained by bacteria via both long-term intracellular uptake (e.g. active assimilation) and passive cell wall adsorption. They also provide insight into the bioprecipitation processes that might occur on the cell walls or in the media due to metabolically induced fluid chemistry changes. In addition, these experiments provide insight into potential element release originating from the bacterial biomass as a result of cell lyses. Duplicate experiments were performed in closed-system 250-mL polypropylene containers with 1 to $8.5\ \text{g}_{\text{wet}}/\text{L}$ rinsed biomass of *P. reactans* HK 31.3 and initial concentrations of Si, Ca, Mg, Fe, Al, Sr, and As ranging from 2 to $3500\ \mu\text{g}/\text{L}$. Three types of aqueous fluids were used: 1) a 0.1 M NaCl and 0.01 M NaHCO_3 solution amended with a 10% NB protein-rich media to allow active bacterial growth and intracellular uptake in cells, 2) the same media with 0.01 M NaN_3 added to prevent bacterial metabolism to assess metal interaction with bacterial cell walls without active assimilation, and 3) a nutrient-free 0.1 M NaCl + 0.01 M NaHCO_3 solution with 0.01 M NaN_3 added to allow cell lysis but minimum element uptake. The typical duration of these experiments was 220 h. The 250-mL polypropylene reactor vessels with biomass were aerated and shaken in the dark at $25\ ^\circ\text{C}$ and periodically sampled. For each sampling, 10 mL

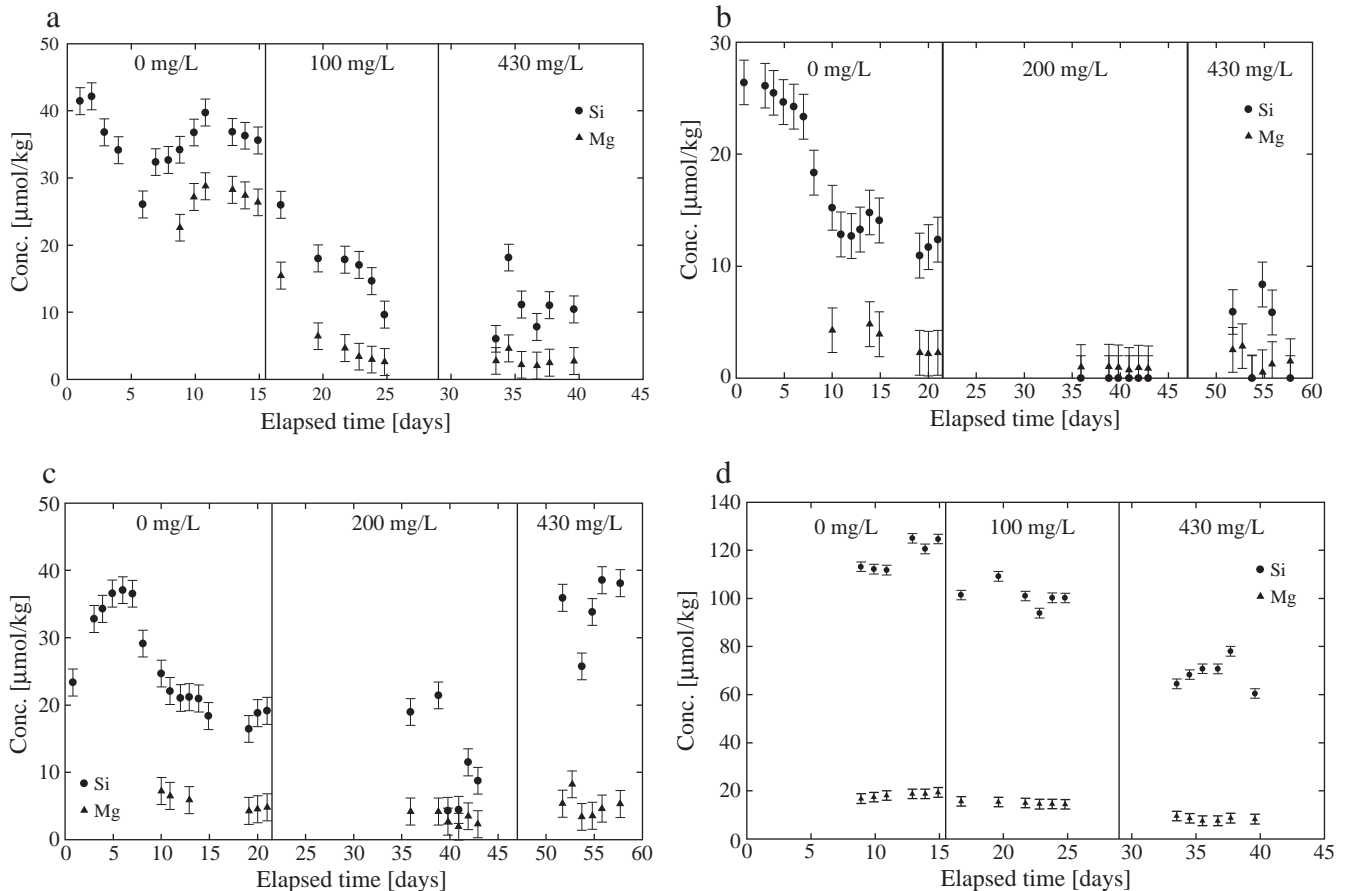


Fig. 3. Total dissolved Si and Mg concentration evolution as a function of time during basaltic glass dissolution experiments with 0, 100 or 200, and 430 $\text{mg}_{\text{wet}}/\text{L}$ dead *Pseudomonas reactans* HK 31.3 added sequentially to the inlet fluid at $25\ ^\circ\text{C}$ and (a) pH -4 (exps. 4-1 to 4-3), (b) pH -6 (exps. 6-10 to 6-12), (c) pH -8 (exps. 8-10 to 8-12), and (d) pH -10 (exps. 10-1 to 10-3). The filled circles and diamonds correspond to measured Si and Mg concentrations. The error bars in these plots correspond to $\pm 2\ \mu\text{mol}/\text{kg}$ uncertainty.

aliquots of homogeneous solution + bacteria were collected using sterile serological pipettes and transferred in sterile polystyrene vials for pH, optical density, bacterial number by agar plate counting. Aqueous metal concentrations were measured in these samples after they were filtered through a 0.45 μm membrane. The biomass/fluid ratio remained constant during experiments and the concentration of bacteria was not affected by the sampling. Sterile controls were routinely run using both nutrient media and 0.01 M NaCl solutions; no bacterial contamination was detected.

3.5. Analytic methods

Filtered solutions were analyzed for all elements using a Agilent 7500 Ion Coupled Plasma Mass Spectrometer (ICP-MS), the 'molybdate blue method' for silicon (Koroleff, 1976), and a Perkin Elmer Zeeman 5000 Atomic Absorption Spectrometer (AAS) for magnesium and aluminum. ICP-MS measurements were made with and without helium gas. Indium and rhenium were used as internal standards, and corrections for oxide and hydroxide ions were made for the rare earth elements (REE) and metals (Ariés et al., 2000). The international geostandard SLRS-4 (Riverine Water Reference Material for Trace Metals certified by the National Research Council of Canada) was used to check the accuracy and reproducibility of each analysis (Yeghicheyan et al., 2001). We obtained good agreement between replicated measurements of SLRS-4 and the certified values (relative difference < 10%), except for B and P (30%).

Selected solid samples were examined using a JEOL 6360 LV and a JEOL JSM840a Scanning Electron Microscope (SEM) after gold or graphite metallization, and by X-ray Photoelectron Spectroscopy (XPS). Energy Dispersive X-ray Spectroscopy (EDS) was used together with SEM to identify primary and secondary mineral phases, and to detect organic signals originating from the bacteria itself or from bacterial processes. XPS analyses used to quantify the stoichiometry of the basaltic glass surface (< 100 Å) layer, were performed using a Kratos Axis Ultra DLD instrument. The excitation energy was a monochromatic AlK α ($h\nu = 1486.6$ eV) at a power of 180 W. The base pressure in the chamber was 5×10^{-10} Torr and never exceeded 5×10^{-9} Torr. A charge balance system was used to compensate for surface charging and for the adventitious carbon. For survey scans, a pass energy of 160 eV and a step size of 0.5 eV was used, and for high resolution scans, these settings were 10 eV and 0.1 eV, respectively. Data interpretation was made with the commercial software CasaXPS, using a Shirley background. The uncertainty for these analysis methods is estimated to 5% for the ICP-MS, 3% for the spectrophotometer, 2% for the AAS analysis, and 10% for the XPS analysis.

4. Experimental results

In total 46 steady-state basaltic glass dissolution experiments were performed in this study. The steady-state fluid chemistry of these 46 experiments is listed according to pH in Tables 3a and 3b, and the

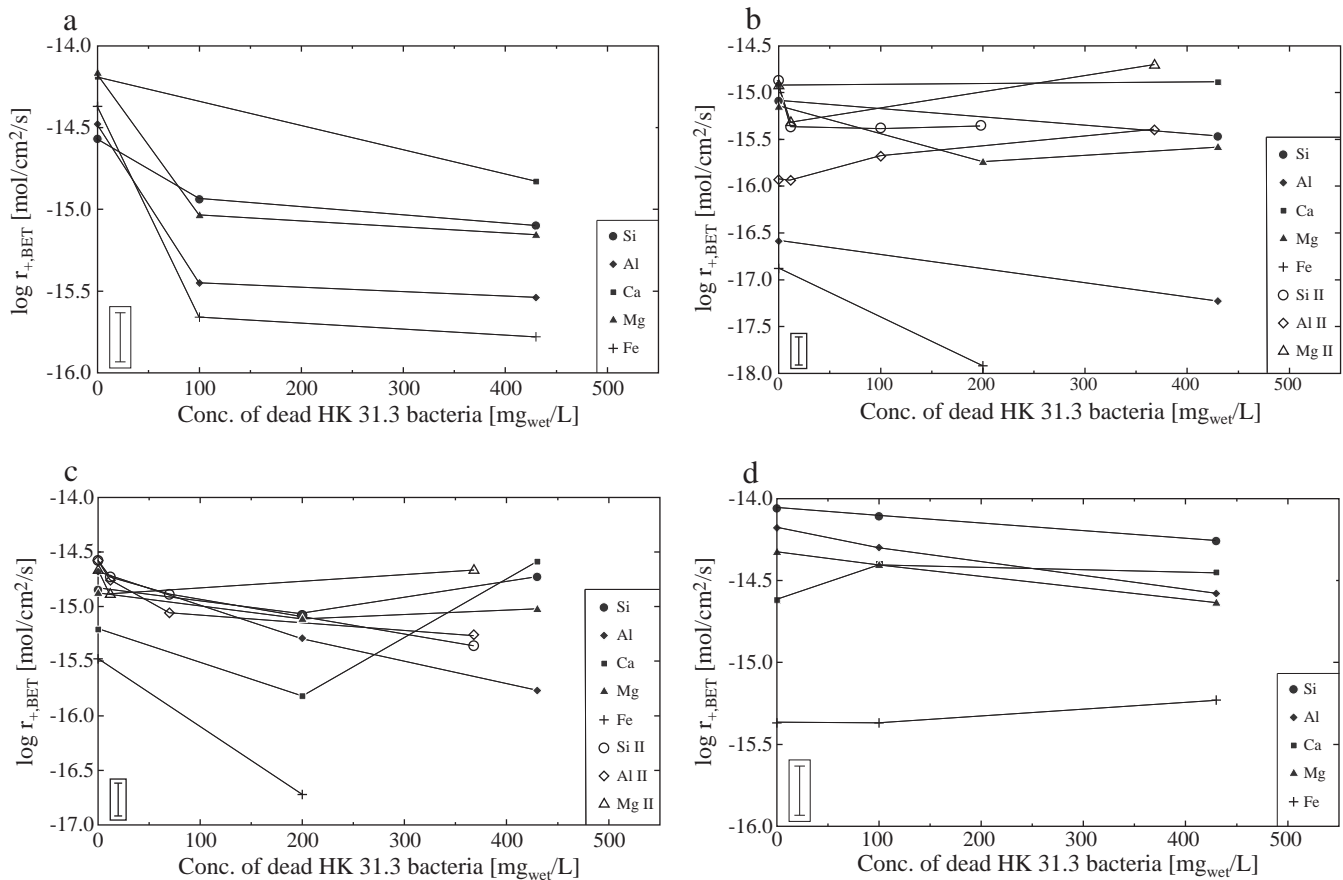


Fig. 4. Measured basaltic glass dissolution rates based on Si, Al, Ca, Mg and Fe during experiments with dead *Pseudomonas reactans* HK 31.3 sequentially added to the inlet fluids at 25 °C and (a) pH ~4 (exps. 4-1 to 4-3), (b) pH ~6 (exps. 6-10 to 6-12, and 6-5 to 6-9), (c) pH ~8 (exps. 8-10 to 8-12, and 8-5 to 8-9), and (d) pH ~10 (exps. 10-1 to 10-3). The symbols are defined in the legend shown in the figure. The error bars in the lower left of each plot correspond to ± 0.15 log units uncertainty on the rates.

main results of these mixed-flow reactor experiments are described in Sections 4.1 and 4.2 below.

4.1. Basaltic glass dissolution in the presence of dead bacteria in BMFR

To test the effect of dead *P. reactans* on the basaltic glass dissolution rates over a broad pH-range, four dissolution experiment series were performed at pH ranging from 4 to 10 at 25 °C (experiments 4-1 to 4-3, 6-10 to 6-12, 8-10 to 8-12, and 10-1 to 10-3). Fig. 3 shows the fluid Si and Mg concentrations originating from basaltic glass dissolution as a function of elapsed time as the dead bacteria concentration was increased. Steady-state Si and Mg concentrations were attained within a few days after the bacteria were added to the system. There was a general trend of a decreasing Si concentration with increasing dead bacteria concentration in each series (see Fig. 3). This effect was less pronounced for Mg. Dissolution rates for these experiments based on the five major elements, Si, Al, Ca, Mg, and Fe are shown in Fig. 4. These plots suggest that the presence of dead bacteria inhibited basaltic glass dissolution rates by as much as a 0.5 log units during experiments 4-1 to 4-3. Some of this decrease likely stems from the shift in outlet solution pH due to cell lysis and organic matter release from the dead cells (see Section 5.1 below). The DOC concentration in the dead bacteria experiments typically varied from 10 to 30 mg/L for the biomass range from 1 to 6.5 g_{wet}/L, suggesting the presence of cell lysis products in the reactive fluids.

PHREEQC modeling of the initial bacteria-free system indicates that Al-phases (i.e. boehmite, diaspore, gibbsite) were supersaturated

in the pH ~4 outlet fluids of experiments 4-1 to 4-3, which could explain, at least in part, the observed decrease in fluid phase Al concentration, when the dead bacteria were added (see Fig. 4a). There is no obvious saturated iron phase that could explain the decrease in Fe, but this could be due to Fe³⁺ and/or FeOH²⁺ adsorption onto dead bacteria surfaces. At pH ~6 (experiments 6-10 to 6-12), both Al- and Fe-hydroxides (i.e. gibbsite, goethite) were highly supersaturated and most likely contributed to the initially low Al and Fe release rates observed in Fig. 4b. However, in an additional experimental series conducted at this pH (experiments 6-5 to 6-9), Al release exhibited slightly increasing rates (see Fig. 4b). The presence of cell lysis products could increase oxy(hydr)oxide solubility via aqueous complexing of Al and Fe with DOC. Unfortunately, this process cannot be quantified due to lack of knowledge of the identity of the organic ligands present and the paucity of metal–ligand stability constants. In contrast to Fe and Al, the Si, Mg and Ca dissolution rates did not show any distinct evolution with increasing dead bacteria concentration at near to neutral pH. According to thermodynamic calculations, the outlet solutions of experiments 10-1 to 10-3 were supersaturated with respect to several secondary phases including calcite, aragonite, gibbsite, kaolinite, smectite, mesolite, natrolite, scolecite, and stilbite. Nevertheless, the results of these pH ~10 experiments showed only a slight decrease in dissolution rates based on Si, Al, and Mg release of 0.2–0.4 log units in the presence of dead bacteria (see Fig. 4d), which is almost within the ±0.15 log unit experimental uncertainty of the combined measurements. The basaltic glass itself was strongly undersaturated in all of the initial bacteria-free experiments with an A* greater than 10 kJ/mol (see Table 3b),

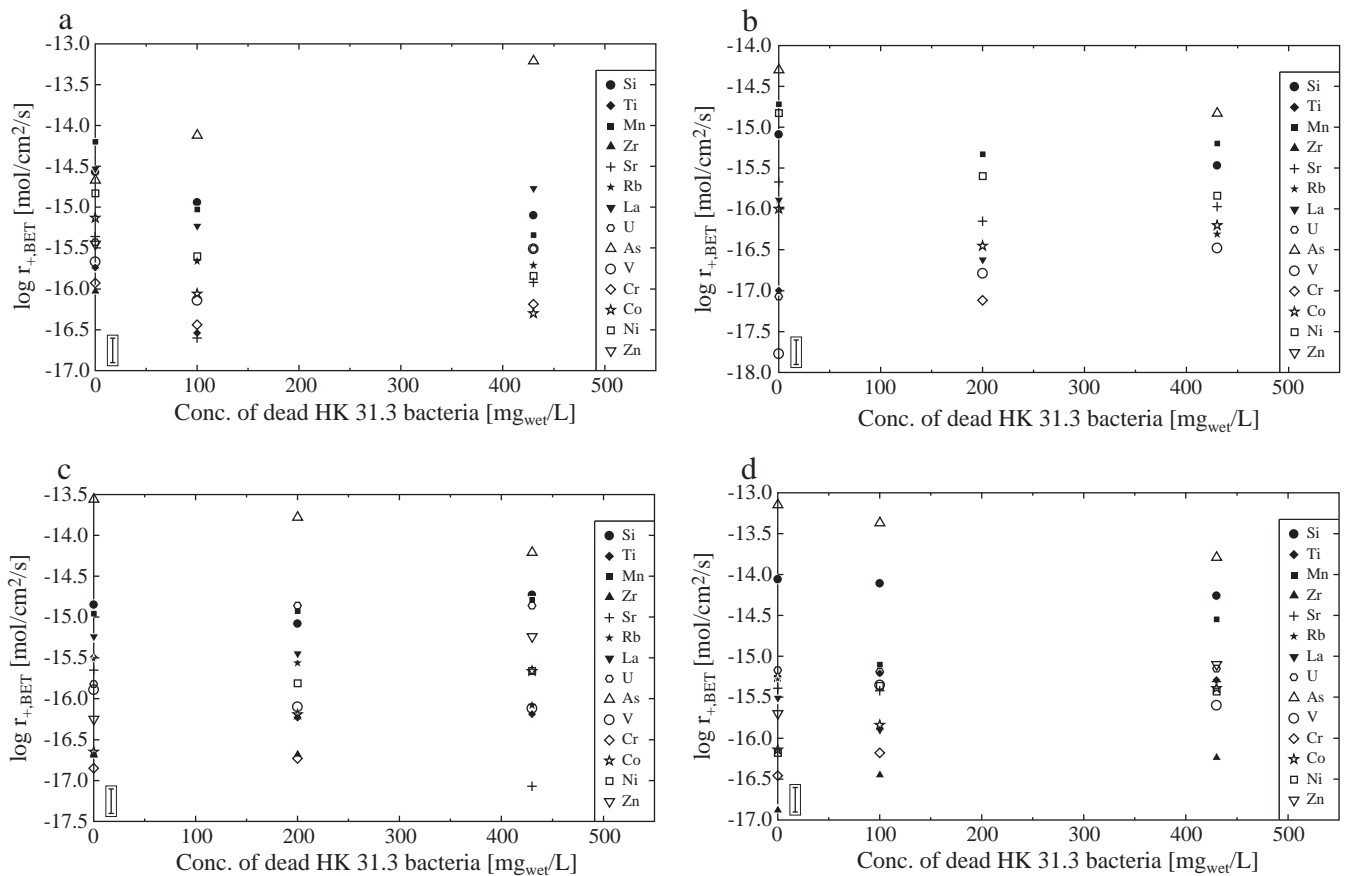


Fig. 5. Measured basaltic glass dissolution rates based on trace element release during experiments with dead *Pseudomonas reactans* HK 31.3 sequentially added to the inlet fluids at 25 °C and (a) pH ~4 (exps. 4-1 to 4-3), (b) pH ~6 (exps. 6-10 to 6-12), (c) pH ~8 (exps. 8-10 to 8-12), and (d) pH ~10 (exps. 10-1 to 10-3). The symbols are defined in the legend shown in the figure. The error bars in the lower right of each plot correspond to ±0.15 log units uncertainty on the rates.

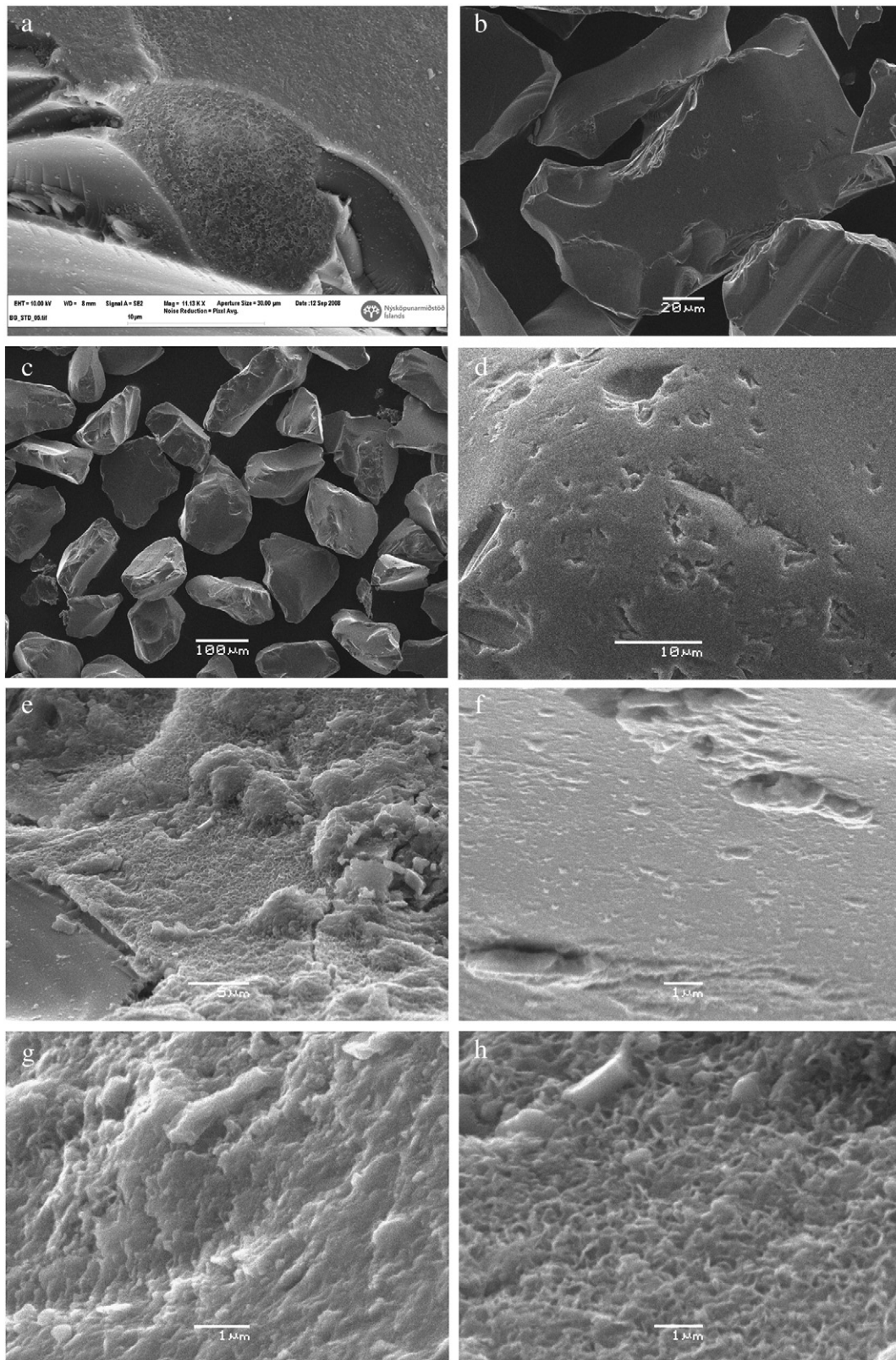


Fig. 6. Scanning Electron images of basaltic glass surfaces: a) basaltic glass surface prior to experiments, b) after experiments 10-1 to 10-3 performed in the presence of dead bacteria, c) and d) after experiments 8-10 to 8-13 performed in the presence of dead bacteria showing rounded particles and dissolution etch pits, e) after experiments E5-1 to E5-3 performed in the presence of live bacteria and nutrients showing biofilm-looking coverage of the surface, f) after experiments E3-1 to E3-3 performed in the presence of live bacteria experiment and nutrients showing bacterial “imprints”, g) and h) close-up of biofilm coverage of glass surfaces after experiments E5-1 to E5-3 and E3-1 to E3-3, respectively.

where A^* refers to the chemical affinity of the hydrated basaltic glass in Eq. (1).

Dissolution rates based on selected trace elements, Ti, Mn, Zr, Sr, Rb, La, U, As, V, Cr, Co, Ni and Zn are plotted on Fig. 5 as a function of fluid phase dead bacteria concentration. Among studied elements, only arsenic (As) at pH ~4 showed increasing release rates, of 0.5–1.5 log units, in the presence of dead bacteria (see Fig. 5a), whereas at pH 8–10, a 0.5-order of magnitude decrease in As release rate was observed (see Fig. 5c, d). Note also that there was an order of magnitude increase of Cr release rates with increasing dead biomass concentration at pH 8–10. Other than for these exceptions, the other trace elements generally showed the same pattern as the major elements. Their rates, however, tend to be lower than those predicted from Si rates and the stoichiometry of basaltic glass (see Table 1). Of the trace elements, only arsenic appeared to have higher stoichiometric release rates than Si based on XRF analysis (see Fig. 5a–d).

SEM photos of the basaltic glass prior to experiments were compared with glass from bacteria-free and post-bacterial experiments in Fig. 6a–d. The only dissolution features evident are etch pits (see Fig. 6d); there is no evidence of a specific effect due to either the dead bacteria or their lysis products. In general, the post-experimental glass surfaces appeared smooth and free of secondary precipitates.

4.2. Basaltic glass dissolution in the presence of live bacteria in BMFR

Similar experiments were performed in the presence of live bacteria. Fig. 7 illustrate the temporal evolution of Si and Mg concentration in

the fluid phase as live bacteria were added to the inlet fluids. Note the presence of live bacteria shifts the inlet fluid pH from pH 4 and 10 towards neutral in the outlet fluid likely due to bacterial metabolism. As such these experiments were only run at pH 6 to 8.7 corresponding to the natural pH range of *P. reactans* growth (Shirokova et al., 2012). Various bacteria concentrations were tested in experiments with and without nutrients added to the inlet fluids to assess the effect of bacterial nutritional status on element release rates from basaltic glass.

No significant decrease in outlet fluid Si concentration was found for experiments with live bacteria (see Fig. 7), except for experiments E5–1 to E5–3 performed with no added nutrients (see Fig. 7a). In this one instance a 50% decrease in Si release rates with increasing bacteria concentration from 0 to 6.5 g_{wet}/L was observed. The release rates of the five major elements of basaltic glass shown in Fig. 8 depicts an interesting effect of nutrient addition. As described above for dead cells, Al- and Fe-hydroxide precipitates are almost unavoidable at pH 6 to 8. However, in the presence of nutrients, basaltic glass dissolution shows almost perfect stoichiometric behavior even at neutral pH. This is interpreted to be a consequence of the presence of organic molecules, originating from the nutrients, which contains peptone or yeast extract, which can complex Al and Fe ions in aqueous solution. This change of aqueous Fe and Al speciation increased the stability of these elements in the fluid phase preventing secondary precipitate formation.

Trace elements follow the same pattern as the major elements in response to the addition of live bacteria (not shown). Mn and Ti are released stoichiometrically when nutrients are added, but the remaining

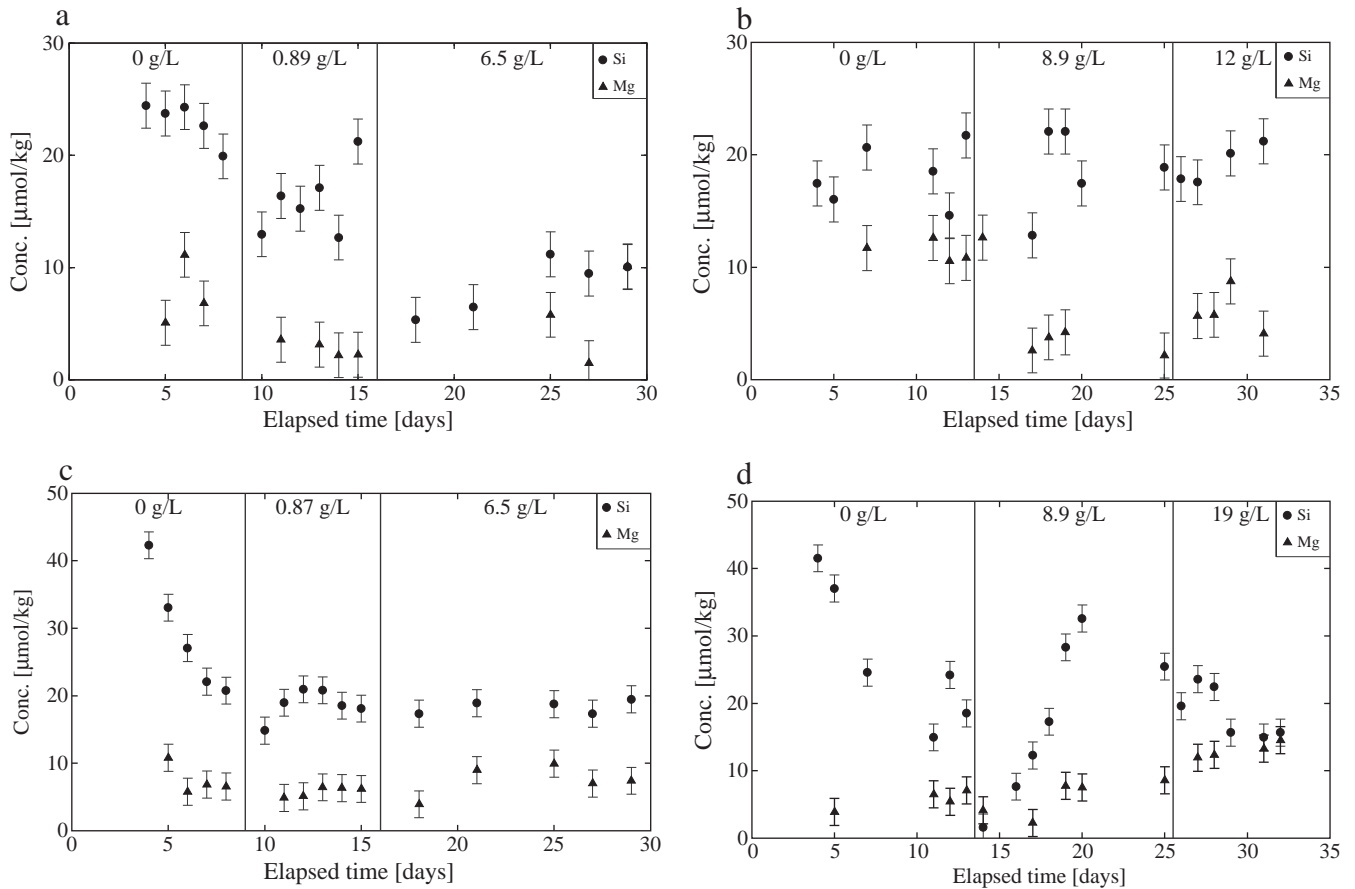


Fig. 7. Total dissolved Si and Mg concentration evolution as a function of time during basaltic glass dissolution experiments in the presence of selected live *Pseudomonas reactans* HK 31.3 concentrations at 25 °C and a) pH 6 to 7 without nutrients (exps. E5-1 to E5-3), b) pH ~7.5 with 10% nutrient broth (exps. E3-1 to E3-3), c) pH 8.5 to 9 without nutrients (exps. E6-1 to E6-3), and d) pH ~8 with 10% nutrient broth (exps. E4-1 to E4-3). The filled circles and diamonds correspond to measured Si and Mg concentrations. The error bars correspond to $\pm 2 \mu\text{mol/kg}$ uncertainty.

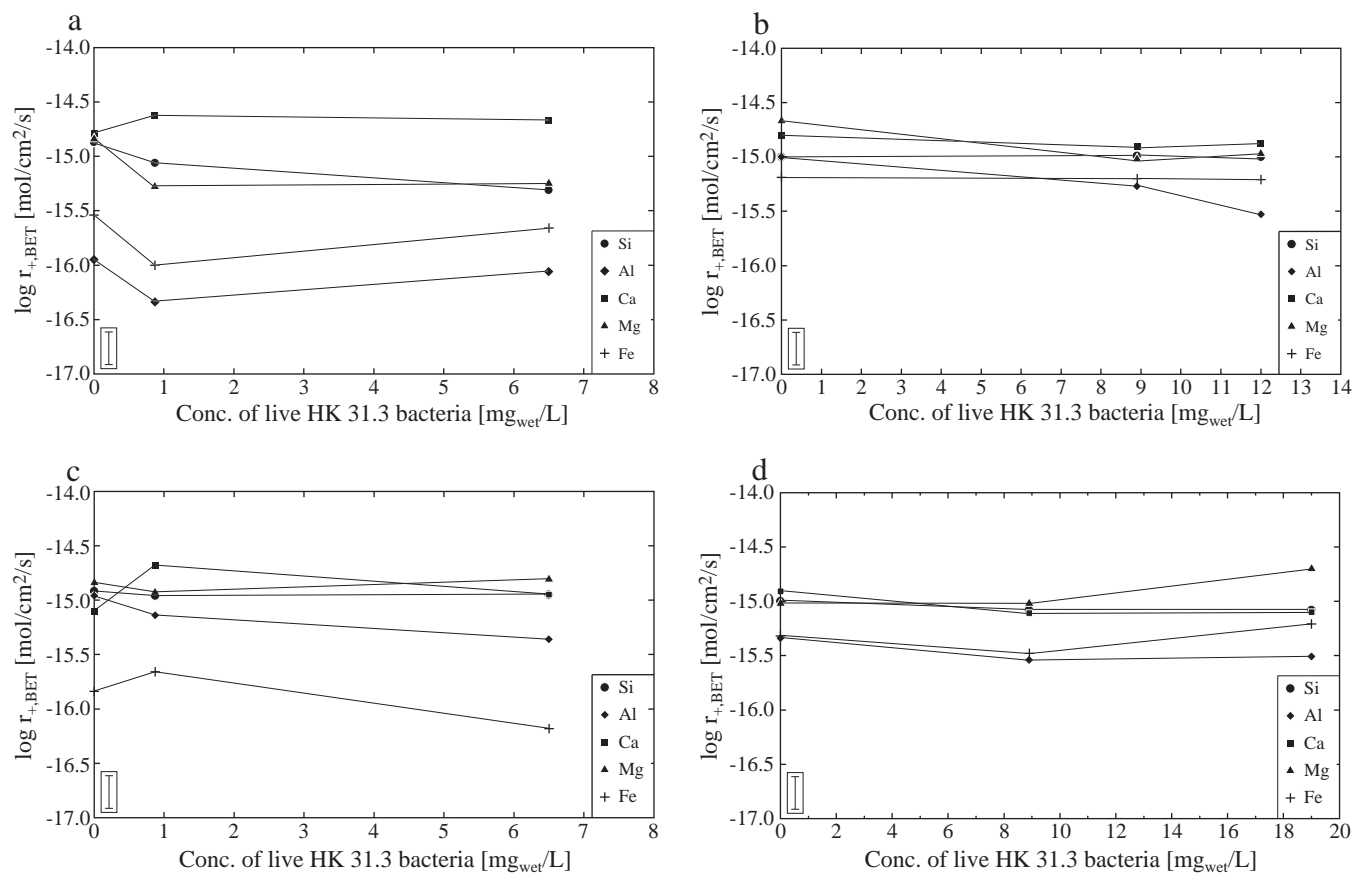


Fig. 8. Measured basaltic glass dissolution rates based on Si, Al, Ca, Mg and Fe release during experiments performed with live *Pseudomonas reactans* HK 31.3 added to the inlet fluids at 25 °C and at a) pH 6 to 7 without nutrients (exps. E5-1 to E5-3), b) pH ~7.5 with 10% nutrient broth (exps. E3-1 to E3-3), c) pH 8.5 to 9 without nutrients (exps. E6-1 to E6-3), and d) pH ~8 with 10% nutrient broth (exps. E4-1 to E4-3). The symbols are defined in the figure. The error bars in the lower right of each plot correspond to ± 0.15 log units uncertainty on the rates.

trace elements do not show any distinct dissolution patterns. Arsenic concentration is below the analytical detection limit (~ 0.01 ppb) for the majority of the live bacteria experiments and therefore no substantial increase in its release rates is observed, in contrast with

the experiments conducted with dead bacteria. The difficulty of quantifying trace element release rates in experiments with live bacteria may result from 1) their uptake by the bacteria (discussed below), 2) analytical uncertainty in the ICP-MS analysis ($\pm 5\%$), or 3) the small

Table 4
Results of X-ray photoemission spectroscopy (XPS) analysis of basaltic glass surfaces.

Sample: ^a	Atomic percentage ratio										
	C/Si	O/Si	Si/Si	Fe/Si	Mg/Si	Ca/Si	Na/Si	Ti/Si	P/Si	Al/Si	N/Si
Basaltic glass original 1	0.22	2.48	1.00	0.08	0.15	0.10	0.01	0.02	0.00	0.35	0.00
Basaltic glass original 2	0.21	2.56	1.00	0.09	0.17	0.09	0.02	0.02	0.00	0.34	0.00
Basaltic glass original av.	0.22	2.52	1.00	0.09	0.16	0.10	0.02	0.02	0.00	0.34	0.00
8-13 ^b											
Post expt. 8-13 live 1	0.59	2.46	1.00	0.05	0.10	0.05	0.04	0.02	0.00	0.34	0.09
Post expt. 8-13 live 2	0.60	2.32	1.00	0.04	0.12	0.06	0.04	0.01	0.00	0.33	0.09
Post expt. 8-13 av.	0.60	2.39	1.00	0.05	0.11	0.06	0.04	0.02	0.00	0.33	0.09
E6-3 ^b											
Post expt. pH 8 live, no nutr. 1	1.74	2.73	1.00	0.06	0.07	0.03	0.01	0.02	0.05	0.45	0.22
Post expt. pH 8 live, no nutr. 2	1.79	2.74	1.00	0.08	0.06	0.04	0.01	0.02	0.07	0.43	0.25
Post expt. pH 8 live, no nutr. av.	1.76	2.73	1.00	0.07	0.07	0.03	0.01	0.02	0.06	0.44	0.23
E4-3 ^b											
Post expt. pH 8 live, 10% nutr. 1	2.66	2.63	1.00	0.04	0.10	0.03	0.00	0.01	0.00	0.39	0.41
Post expt. pH 8 live, 10% nutr. 2	2.49	2.47	1.00	0.04	0.11	0.03	0.00	0.01	0.00	0.40	0.36
Post expt. pH 8 live, 10% nutr. av.	2.57	2.55	1.00	0.04	0.10	0.03	0.00	0.01	0.00	0.40	0.38

^a There is a duplicate ('2') of each analysis, and the average is listed in the line marked "sample name" and "av."

^b Refers to exp. names in Tables 3a–3b.

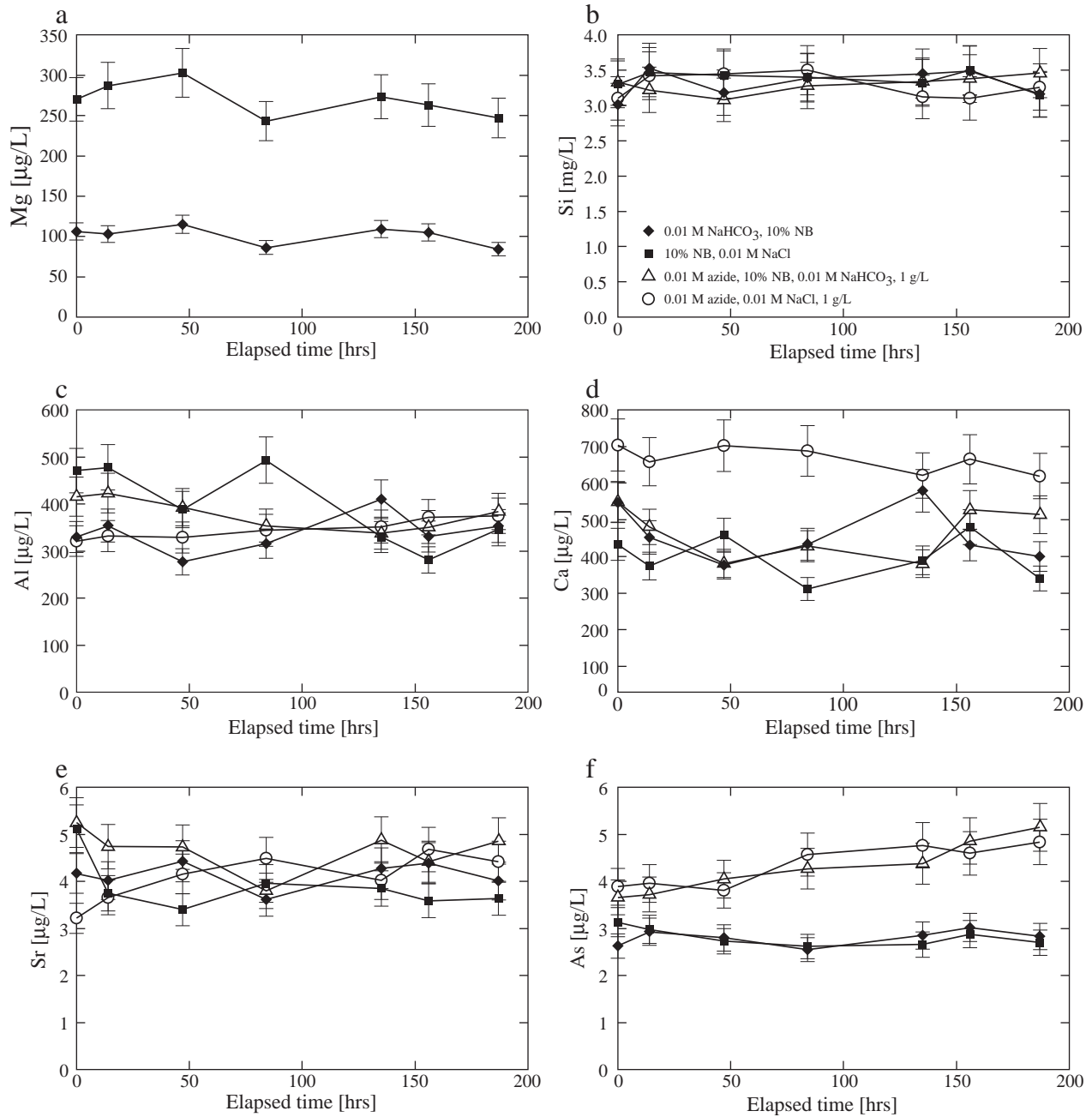


Fig. 9. Temporal evolution of dissolved Mg, Si, Al, Ca, Sr, and As concentration in closed system mineral-free experiments with live bacteria performed in an aqueous 0.01 M NaCl, 10% NB inlet fluid, and inactivated bacteria performed in an aqueous 0.01 M NaN_3 inlet fluid. The biomass concentration increased from 0.1 to 1.2 $\text{g}_{\text{wet}}/\text{L}$ for live bacteria experiments (black diamonds and squares) and stayed constant at 1 $\text{g}_{\text{wet}}/\text{L}$ for inactivated bacteria (white triangles and circles). The error bars correspond to the estimated uncertainty and reproducibility of the measurements, which ranged from 7 to 10%.

difference between the inlet and outlet concentration of these elements at steady-state. In any case, it is clear that the presence of live bacteria does not lead to any large increases ($\geq 30\%$) in trace element release rates from basaltic glass into the fluid compared to bacteria-free experiments.

SEM images of basaltic glass samples collected after the live bacteria experimental series show the presence of a biofilm-looking layer on the glass surfaces (see Fig. 6e). Furthermore, some surface features suggestive of bacterial imprints are observed (see Fig. 6f) which contrast to typical dissolution features such as etch pits (see Fig. 6d). However, this biofilm-like layer is patchy and heterogeneous as most surfaces appear clear and smooth.

Results of post-experimental basaltic glass surface analysis by XPS provided in Table 4 show a depletion in surface Fe, Mg, and Ca concentration, consistent with cation leaching, and some Al enrichment, perhaps in the form secondary phases, not explicitly identified during SEM analyses. An enrichment in C and N, especially in experiments performed at pH ~ 8 with live cultures in nutrient media, confirms the presence of biofilms as inferred from the SEM observations (see Fig. 6e, g, h).

BET surface area measurements of the basaltic glass at the end of experiments with live bacteria yielded the value close to $3000 \text{ cm}^2/\text{g}$, which is $\sim 50\%$ lower than the initial BET surface area. It supports the observations made by comparing various SEM images that the

basaltic glass grains were smoothed and rounded during the experiments. There is therefore no indication that the presence of live *P. reactans* increased specific surface area.

4.3. Element assimilation and release by bacteria cells in basaltic glass free, closed-system batch experiments

The temporal evolution of fluid phase Mg, Ca, Al, Si, and trace element concentrations in basaltic glass-free, closed-system batch experiments with live and dead bacteria and in nutrient-free media is shown in Fig. 9; a summary is provided in the electronic annex. In Mg-poor fluids (100–300 $\mu\text{g/L}$) and nutrient-rich media there is a $\leq 10\%$ decrease of Mg concentration, likely due to intracellular uptake of this element. Extrapolating these results to the typical bacterial concentrations used in the experiments suggest that $\leq 1 \mu\text{mol/L}$ of the Mg released to solution by basaltic glass dissolution was consumed by bacterial cells via intracellular uptake. The Si concentration evolution during bacterial growth does not exhibit a systematic variation within the experimental uncertainty (see Fig. 9b) confirming that Si uptake/adsorption and release due to cell lysis are negligible at the investigated conditions. The uptake of Ca, Mg, and Sr was also small and within the experimental reproducibility of 20–30%. The Al concentration did not exhibit any systematic change during of bacterial growth, although the assimilation of 100 $\mu\text{g Al/g}_{\text{wet}}$ was observed in nutrient-bearing 0.01 M NaCl solution (see Fig. 9c). Bacterial uptake of As was absent, but there was a small release of As from the inactivated biomass with 1 $\mu\text{g As/g}_{\text{wet}}$ over ~ 190 h. Taken together these results suggest that bacterial absorption and bacterial uptake play a minor role in the BMFR experiments performed in this study. Thus the observed changes in chemical composition of the solutions in the BMFR experiments mainly stems from dissolution of the basaltic glass.

5. Discussion

5.1. The effect of cell wall adsorption and bacterial assimilation on mass balance calculations

The elemental constituents released from the glass surface in the presence of bacteria can be incorporated into: (i) the $<0.45 \mu\text{m}$ fluid fraction consisting of ions and molecules, simple organic complexes, and organic colloids of the lysis products and cell exometabolites; (ii) cell wall surfaces via adsorption, and (iii) bacteria interiors via assimilation (e.g. Hutchens et al., 2003; Neaman et al., 2005a,b, 2006). Whereas the mass of released elements incorporated into the fluid fraction was measured directly after these fluids were passed through

$0.45 \mu\text{m}$ filters, the mass incorporated into cell walls or into bacteria could only be estimated via bacterial growth experiments in basaltic glass-free, Mg, Ca, Al, Si-bearing solutions. Measurement of the Mg, Ca, and Al desorbed from the cell surface upon EDTA treatment suggests that less than 20% of all elements released from our basaltic glass dissolution experiments were incorporated into cell walls or the bacteria interiors. As such this contribution to mass balance was neglected when calculating rates whose typical uncertainty was $\pm 0.1 \log R$ units.

5.2. Effect of nutrients and bacteria on basaltic glass element release rates

The degree to which the presence of bacteria affects basaltic glass dissolution rates can be assessed with the aid of Fig. 10. Rates measured in the absence of bacteria are for the most part consistent with corresponding dissolution rates reported for this glass by Oelkers and Gislason (2001). Further comparison of Si release rates obtained in this and previous studies is shown in Table 5. The results shown in this table confirm that the rates obtained in this study are consistent with previous results (Oelkers and Gislason, 2001; Gislason and Oelkers, 2003; Stockmann et al., 2011).

Within the scatter of the data, the effect of the presence of either live or dead *P. reactans* is identical; rates in the presence of *P. reactans* are on average 0.3 log units lower than corresponding rates measured in bacteria-free experiments. This observation suggests that the influence of metabolic activity on basaltic glass dissolution rates at our experimental conditions is small. Note the average 0.3 log unit difference between rates measured in biotic versus abiotic experiments are within the combined uncertainty of the respective rate measurements.

Since both “starving” and “healthy” bacteria were tested (in nutrient-free and nutrient-rich media) over a wide range of biomass concentration, we suggest our experiments cover the likely range of conditions found in natural systems and as such these results can be extrapolated to basaltic glass during natural weathering.

There are several possible reasons why the presence of bacteria affects negligibly basaltic glass dissolution rates. First, the attachment of *P. reactans* exometabolites to basaltic glass surfaces may not be sufficient to facilitate the rupture of Si–O bonds, the main rate-controlling factor of glass dissolution. Moreover such effects may be balanced by the inhibiting effects of bacterial attachment blocking active sites on the basaltic glass surface; bacterial biofilm formation on surfaces is known to inhibit dissolution (Welch and Vandevivere, 1994; Ullman et al., 1996; Buchardt et al., 2001; Hutchens et al., 2006; Davis et al., 2007; Aouad et al., 2008; Hutchens, 2009; Hutchens et al., 2010), and the excretion of complex polysaccharides may also decrease dissolution rates (Welch and Vandevivere, 1994; Welch et al., 1999). It has also been suggested that microbially mediated dissolution may be less effective when bacteria are in direct contact with mineral surfaces (Hutchens et al., 2006). For example, a typical environmental bacterium, *Shewanella oneidensis* MR-1 was reported to decrease calcite dissolution rates via biofilm formation by inhibiting etch pit formation at screw or point dislocations (Lüttge and Conrad, 2004).

5.3. Comparison with literature data on the effect of bacteria on silicate minerals dissolution

Over the past decades, extensive research has focused on the effect of organic ligands on mineral dissolution rates (Ganor et al., 2009; Pokrovsky et al., 2009 and references therein). However, in contrast to our relatively good understanding of the effect of the presence of organic ligands on Ca, Mg-bearing silicate dissolution rates, there is relatively little quantitative literature data on the effect of bacteria on these rates. For example, it has been shown that a soil strain of *Pseudomonas* is capable of producing 2-ketogluconic acid from glucose and thus promoting the dissolution of the Ca, Zn, Mg silicates, wollastonite, apophyllite and olivine via formation of Ca-2 ketogluconate (Webley et al., 1960;

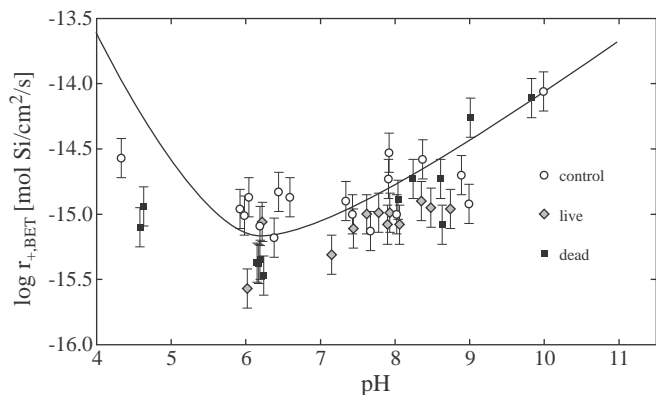


Fig. 10. Variation of measured steady-state BET normalized basaltic glass dissolution rates based on Si release as a function of pH. The symbols correspond to rates measured in the present study whereas the curve was generated from equations and parameters reported by Oelkers and Gislason (2001) for a total aqueous Al concentration of 10^{-6} mol/kg.

Table 5Steady-state Stapafell basaltic glass dissolution rates obtained from abiotic experiments at 25 °C reported from various sources. All rates are given in units of mol/cm²/s.

pH	Log $r_{+,Si,BET}^a$	Log $r_{+,Si,geo}^a$	Log $r_{+,Si,BET}^b$	Log $r_{+,Si,geo}^b$	pH ^c	Log $r_{+,Si,BET}^c$	Log $r_{+,Si,geo}^c$	pH ^d	Log $r_{+,Si,BET}^d$	Log $r_{+,Si,geo}^d$	Log $r_{+,Ca,Mg,BET}^{d,e}$	Log $r_{+,Ca,Mg,geo}^{d,e}$
4.5			–14.2	–12.2				4.3	–14.6	–13.2	–14.2	–12.8
6.0	–15.2	–13.2	–15.0	–13.0				6.0	–15.0	–13.6	–14.9	–13.6
6.5			–15.0	–13.0				6.6	–14.9	–13.5	–14.8	–13.4
7.0	–15.1	–13.1	–14.9	–12.9	7.0	–15.1	–13.7					
8.0	–14.8	–12.8	–14.6	–12.6	7.9	–14.7	–13.3	7.9	–14.6	–13.3		
8.5			–14.4	–12.4	8.6	–14.8	–13.4	8.4	–14.6	–13.2	–14.7	–13.3
9.0	–14.4	–12.4	–14.2	–12.2				8.9	–14.8	–13.4	–15.0	–13.6
10.0	–14.1	–12.1	–13.9	–11.9	10.1	–14.3	–13.0	10.0	–14.1	–12.7	–14.3	–13.0

^a From Oelkers and Gislason (2001).^b From Gislason and Oelkers (2003). A roughness factor of 92 is used to calculate $r_{+,geo}$ from $r_{+,BET}$.^c From Stockmann et al. (2011). The basaltic glass roughness factor is 23.^d This study, bacteria- and nutrient-free experiments.^e This study, average of Ca and Mg dissolution rates. For the pH 10.0 experiment, only Mg rates are given.

Duff et al., 1962; Webley et al., 1963); however, no quantitative description of the process were generated. A recent study of soil rhizospheric bacteria *Pseudomonas aureofaciens* suggests these bacteria have little effect on wollastonite dissolution rates both in nutrient-free and nutrient-rich solutions (Pokrovsky et al., 2009). Fayalite (Fe₂SiO₄) dissolution at pH = 2 in the presence of acidophilic, iron-oxidizing bacteria was significantly inhibited compared to abiotic controls (Santelli et al., 2001). This inhibition was attributed to formation of unreactive laihunite-like (Fe²⁺+Fe³⁺)₂(SiO₄)₂ surface regions due to bacterial oxidation of released Fe²⁺ (Welch and Banfield, 2002). Such mechanisms, however, are unlikely to occur at the conditions of our experiments because of they were performed at higher pH, and, as a result, significantly lower dissolved Fe concentration.

xAluminosilicates and Fe-bearing minerals are generally considered to be much more susceptible to microbial-promoted dissolution than Ca, Mg-bearing orthosilicates (see Berner, 2010; Pokrovsky et al., 2010 for discussion). The main reason is the change of aqueous Al and Fe speciation due to the presence of bacterial exometabolites and siderophores. Aqueous complexation decreases the activity of aqueous Al³⁺ and Fe³⁺, which (i) avoids secondary mineral formation, (ii) increases overall dissolution rates (Welch and Ullman, 1993; Vandevivere et al., 1994; Oelkers and Schott, 1998; Liermann et al., 2000a,b; Maurice et al., 2001) and (iii) increases the selective uptake of trace metals (Brantley et al., 2001). It is also worth noting that despite a common belief that microbes accelerate weathering (Robert and Berthelin, 1986; Thorseth et al., 1992; Uroz et al., 2009), there are numerous studies that conclude this effect is either rather weak or inhibiting (see Valsami-Jones and McEldowney, 2000; Balogh-Brunstad et al., 2008; Hopf et al., 2009; Hutchens, 2009; Sverdrup, 2009).

5.4. Application to subsurface CO₂ storage and soil weathering

The results of this study provide insight into the potential impact of heterotrophic bacteria on basaltic glass dissolution and during subsurface CO₂ storage efforts. Typical concentrations of live *P. reactans* cells used in the experiments presented above are 10⁷–10⁸ cells/mL. This is 6 orders of magnitude higher than the total concentration of culturable heterotrophic aerobic bacteria measured in the Icelandic groundwater samples used to separate *P. reactans* ($n \cdot 10 - n \cdot 100$ CFU/mL, Shirokova et al., 2009). However, the bacterial concentrations considered in our experiments are comparable with i) average bacterial populations in soils, which commonly range from 10⁶ to 10⁹ cells/cm³ (Atlas and Bartha, 1993), ii) bacterial concentrations in shallow aquifers (10⁶ cells/mL, Ehrlich, 1996), and (iii) in deep subsurface environments (Sinclair and Ghiorse, 1989; Stevens and McKinley, 1995; Pedersen, 1997). Although culturable bacteria represent only a small proportion of the species present in natural systems (e.g. Pedrós-Alió, 2006), the high concentrations of bacteria used in this

present study allow straightforward evaluation of the degree to which the heterotrophic bacteria are capable of influencing glass dissolution in natural settings.

The relatively weak effect of bacteria and microbial exometabolites on basaltic glass observed in this study, together with similar observations on olivine (Shirokova et al., 2012), and other Ca–Mg-bearing silicates such as wollastonite (Pokrovsky et al., 2009) suggests that the impact of heterotrophic aerobic culturable bacteria on “basic” mineral and aluminosilicates chemical weathering rates in soils and during carbon sequestration efforts may be weaker than generally thought.

6. Conclusions

The experiments presented above show that the presence of live or dead bacteria affects only mildly basaltic glass dissolution rates based on Si release; constant pH rates were observed in this study to decrease by no more than a factor of 3 in the presence of *P. reactans*. Other major cations including Al, Ca, Mg, and Fe exhibit a similar behavior. A decrease in Al concentration due to the presence of *P. reactans* was observed in nearly all of the experiments. Al might be adsorbed on bacteria surfaces, but little aqueous Al-complexing with bacteria and exometabolites is indicated by the lack of acceleration in basaltic glass dissolution rates in their presence. The presence of nutrient components in solution prevented Al³⁺ and Fe³⁺ from forming secondary precipitates, most likely through organic molecular complexation. No increase of trace elements release from basaltic glass was observed, except for an increase in arsenic release rates at pH 4 in the presence of dead *P. reactans*. As little effect of their presence was found on laboratory dissolution rates it seems likely that *P. reactans* will have a little effect on basaltic glass dissolution rates during either soil weathering or subsurface CO₂ storage efforts in basalts.

Acknowledgments

We would like to thank several colleagues for their help, in particular Carole Causserand, Alain Castillo, and Phillippe de Parseval for technical assistance, and Therese K. Flaathen, Allison Stephenson, Sam Parry, Irina Bundeleva, Quentin Gautier, Giuseppe Saldi, Chris Pearce and Vasileios Mavromatis for lab assistance. Erik Sturkell is gratefully acknowledged for his graphical assistance and continued support. The Environmental and Energy Fund of Reykjavík Energy, the Research Fund of the University of Iceland, the Nordic Council of Ministers through NORDVULK, and the European Community through the MIN-GRO Research and Training Network (MRTN-CT-2006-035488) and the ERASMUS student mobility program are gratefully acknowledged for their financial support. Finally, we would like to thank Editor Jeremy Fein for his valuable comments, which greatly improved this manuscript.

Appendix 1. Chemical composition of the inlet fluids used in the BMFR experiments

Exp.	Inlet fluid (mol/kg)	Ionic strength (mol/kg)	Inlet pH (25 °C)	STDEV pH _{in}	Outlet pH (25 °C)	STDEV pH _{out}	Bacteria (mg _{wet} /L)	Bacteria status ^d	Nutrient (%)
4-1	0.003 m NaOOCCH ₃ + 0.003 m NaCl + 0.003 m HCl	0.009	4.07	0.02	4.33	0.19	0		0
4-2	0.003 m NaOOCCH ₃ + 0.003 m NaCl + 0.003 m HCl	0.009	4.58	0.04	4.63	0.19	100	Dead	0
4-3	0.003 m NaOOCCH ₃ + 0.003 m NaCl + 0.003 m HCl	0.009	4.28	0.06	4.58	0.04	430	Dead	0
4-4	0.003 m NaOOCCH ₃ + 0.003 m NaCl + 0.003 m HCl	0.009	4.18		7.28	1.43	700	Live	0
6-1	0.00998 m NH ₄ Cl + 0.000003 m NH ₄ OH	0.010	5.86	0.15	5.92	0.10	0		0
6-2	0.00998 m NH ₄ Cl + 0.000003 m NH ₄ OH	0.010	5.81	0.02	5.98	0.03	0		0
6-3	0.00998 m NH ₄ Cl + 0.000003 m NH ₄ OH	0.010	6.22	0.10	6.38	0.06	0		1
6-4	0.00998 m NH ₄ Cl + 0.000003 m NH ₄ OH	0.010	6.33	0.06	6.44	0.06	0		10
6-5 ^a	0.001 m MES + 0.0004 m NaOH	0.001	6.05	0.01	6.04	0.04	0		0
6-6 ^a	0.001 m MES + 0.0004 m NaOH	0.001	6.12	0.01	6.15	0.03	11.8	Dead	0
6-7 ^a	0.001 m MES + 0.0004 m NaOH	0.001	6.12	0.01	6.17	0.02	100	Dead	0
6-8 ^a	0.001 m MES + 0.0004 m NaOH	0.001	6.16		6.19	0.02	198	Dead	0
6-9 ^a	0.001 m MES + 0.0004 m NaOH	0.001	6.40		6.39	0.01	368	Dead	0
6-10 ^a	0.001 m MES + 0.0004 m NaOH	0.001	6.10	0.04	6.19	0.05	0		0
6-11 ^a	0.001 m MES + 0.0004 m NaOH	0.001	6.23	0.04	6.32	0.03	200	Dead	0
6-12 ^a	0.001 m MES + 0.0004 m NaOH	0.001	6.10	0.03	6.24	0.02	430	Dead	0
6-13 ^a	0.001 m MES + 0.0004 m NaOH	0.001	6.08		6.15	0.12	700	Live	0
E5-1 ^a	0.01 m MES	0.01	n.m.		6.59	0.14	0		0
E5-2 ^a	0.01 m MES	0.01	n.m.		6.22	0.10	870	Live	0
E5-3 ^a	0.01 m MES	0.01	n.m.		7.15	0.25	6500	Live	0
E3-1 ^a	0.01 m MES	0.01	n.m.		7.43	0.23	0		10
E3-2 ^a	0.01 m MES	0.01	n.m.		7.78	0.07	8900	Live	10
E3-3 ^a	0.01 m MES	0.01	n.m.		7.62	0.13	12,000	Live	10
8-1 ^b	0.0096 m NH ₄ Cl + 0.0004 m NH ₄ OH	0.010	7.92	0.02	7.92	0.03	0		0
8-2 ^b	0.0096 m NH ₄ Cl + 0.0004 m NH ₄ OH	0.010	7.94	0.01	7.91	0.02	0		0
8-3 ^b	0.0096 m NH ₄ Cl + 0.0004 m NH ₄ OH	0.010	7.83	0.09	7.34	0.25	0		1
8-4 ^b	0.0096 m NH ₄ Cl + 0.0004 m NH ₄ OH	0.010	7.89	0.08	7.47	0.25	0		10
8-5	0.01 m NaHCO ₃	0.010	8.55	0.02	8.37	0.06	0		0
8-6	0.01 m NaHCO ₃	0.010	8.46	0.03	8.24	0.07	12	Dead	0
8-7	0.01 m NaHCO ₃	0.010	8.33	0.13	8.04	0.06	70	Dead	0
8-8	0.01 m NaHCO ₃	0.010	8.55		8.04	0.06	195	Dead	0
8-9	0.01 m NaHCO ₃	0.010	8.10		8.01	0.13	368	Dead	0
8-10	0.01 m NaHCO ₃	0.010	8.55	0.04	8.89	0.02	0		0
8-11	0.01 m NaHCO ₃	0.010	8.57	0.11	8.63	0.08	200	Dead	0
8-12	0.01 m NaHCO ₃	0.010	8.36	0.16	8.61	0.08	430	Dead	0
8-13	0.01 m NaHCO ₃	0.010	8.53		8.09	0.27	700	Live	0
E6-1	0.01 m NaHCO ₃	0.010	n.m.		8.99	0.04	0.0		0
E6-2	0.01 m NaHCO ₃	0.010	n.m.		8.74	0.11	870	Live	0
E6-3	0.01 m NaHCO ₃	0.010	n.m.		8.48	0.15	6500	Live	0
E4-1	0.01 m NaHCO ₃	0.010	n.m.		8.02	0.04	0.0		10
E4-2	0.01 m NaHCO ₃	0.010	n.m.		8.06	0.06	8900	Live	10
E4-3	0.01 m NaHCO ₃	0.010	n.m.		7.90	0.10	19,000	Live	10
10-1	0.003 m Na ₂ CO ₃ + 0.004 m NaHCO ₃	0.013	10.05	0.00	9.99	0.04	0		0
10-2	0.003 m Na ₂ CO ₃ + 0.004 m NaHCO ₃	0.013	10.02	0.01	9.83	0.12	100	Dead	0
10-3	0.003 m Na ₂ CO ₃ + 0.004 m NaHCO ₃	0.013	9.94	0.17	9.01	0.33	430	Dead	0
10-4	0.003 m Na ₂ CO ₃ + 0.004 m NaHCO ₃	0.013	10.11		8.37	0.45	700	Live	0

n.m. = not measured.

^a MES is an organic buffer with the chemical composition C₆H₁₃NO₄S.

^b N₂ was bubbled through the inlet solution for 30 min prior to use to minimize the amount of dissolved CO₂ in solution.

Appendix 2. Supplementary data

Supplementary data to this article can be found online at doi:10.1016/j.chemgeo.2011.12.011.

References

- Alfredsson, H.A., Hadrarson, B.S., Franzson, H., Gislason, S.R., 2008. CO₂ sequestration in basaltic rock at the Hellisheidi site in SW Iceland: stratigraphy and chemical composition of the rocks at the injection site. *Mining Magazine* 72, 1–5.
- Aouad, G., Crovisier, J.-L., Geoffroy, V.A., Meyer, J.-M., Stille, P., 2006. Microbially-mediated glass dissolution and sorption of metals by *Pseudomonas aeruginosa* cells and biofilm. *Journal of Hazardous Materials B* 136, 889–895.
- Aouad, G., Crovisier, J.-L., Damidot, D., Stille, P., Hutchens, E., Mutterer, J., Meyer, J.-M., Geoffroy, V.A., 2008. Interactions between municipal solid waste incinerator bottom ash and bacteria (*Pseudomonas aeruginosa*). *The Science of the Total Environment* 393, 385–393.
- Ariés, S., Valladon, M., Polvé, M., Dupré, B., 2000. A routine method for oxide and hydroxide interference corrections in ICP-MS chemical analysis of environmental and geological samples. *Geostandards Newsletter* 24, 19–31.
- Atlas, R.M., Bartha, R., 1993. *Microbial Ecology: Fundamentals and Applications*. Benjamin/Cummings, Redwood City, Canada. 563 pp.
- Bailey, B., Templeton, A., Staudigel, H., Tebo, B.M., 2009. Utilization of substrate components during basaltic glass colonization by *Pseudomonas* and *Shewanella* isolates. *Geomicrobiology Journal* 26, 648–656.
- Balogh-Brunstad, Z., Keller, C.K., Dickinson, J.T., Stevens, F., Li, C.Y., Bormann, B.T., 2008. Bi-otite weathering and nutrient uptake by ectomycorrhizal fungus, *Suillus tomentosus*, in liquid-culture experiments. *Geochimica et Cosmochimica Acta* 72, 2601–2618.
- Belkanova, N.P., Karavaiko, G.I., Avakyan, Z.A., 1985. Cleavage of the syloxane bond in quartz by *Bacillus mucilaginosus*. *Microbiology* 54, 27–30 (in Russian).
- Belkanova, N.P., Eroschev-Shak, V.A., Lebedeva, E.V., Karavaiko, G.I., 1987. Dissolution of kimberlite minerals by heterotrophic microorganisms. *Microbiology* 56, 613–620 (in Russian).
- Benedetti, M.F., Dia, A., Riotte, J., Chabaux, F., Gérard, M., Boulègue, J., Fritz, B., Chauvel, C., Bulourde, M., Déruelle, B., Ildefonse, P., 2003. Chemical weathering of basaltic lava flows undergoing extreme climatic conditions: the water geochemistry record. *Chemical Geology* 201, 1–17.
- Bennett, P.C., Casey, W.H., 1994. Organic acids and the dissolution of silicates. In: Pittman, E.D., Lewan, M. (Eds.), *The Role of Organic Acids in Geological Processes*. Springer-Verlag, New York, pp. 162–201.
- Bennett, P.C., Rogers, J.R., Choi, W.J., 2001. Silicates, silicate weathering, and microbial ecology. *Geomicrobiology Journal* 18, 3–19.
- Berner, R.A., 2010. Comment: effect of organic ligands and heterotrophic bacteria on Wollastonite dissolution kinetics. *American Journal of Science* 310, 424.
- Bourcier, W.L., Peiffer, D.W., Knauss, K.G., McKeegan, K.D., Smith, D.K., 1990. A kinetic model for borosilicate glass dissolution based on the dissolution affinity of a surface alteration layer. *Materials Research Society Symposium Proceedings* 176, 209–216.
- Brantley, S., Liermann, L., Bau, M., 2001. Uptake of trace metals and rare earth elements from hornblende by a soil bacterium. *Geomicrobiology Journal* 18, 37–61.
- Buchardt, B., Israelson, C., Seaman, P., Stockmann, G., 2001. Ikaite Tufa Towers in Ikka Fjord, southwest Greenland: their formation by mixing of seawater and alkaline spring water. *Journal of Sedimentary Research* 71, 176–189.

- Davis, K.J., Neelson, K.H., Lüttge, A., 2007. Calcite and dolomite dissolution rates in the context of microbe–mineral surface interactions. *Geobiology* 5, 191–205.
- Duff, R.B., Webley, D.M., Scott, R.O., 1962. Solubilization of minerals and related materials by 2-ketogluconic acid-producing bacteria. *Soil Science* 95, 105–114.
- Edwards, K.J., Bach, W., McCollom, T.M., Rogers, D.R., 2004. Neutrophilic iron-oxidizing bacteria in the ocean: their habitats, diversity, and roles in mineral deposition, rock alteration, and biomass production in the deep-sea. *Geomicrobiology Journal* 21, 393–404.
- Ehrlich, H.L., 1981. The geomicrobiology of silica and silicates. In: Ehrlich, H.L. (Ed.), *Geomicrobiology*, 2nd ed. Marcel Dekker, Inc., New York, pp. 131–135.
- Ehrlich, H.L., 1996. How microbes influence mineral growth and dissolution. *Chemical Geology* 132, 5–9.
- Fein, J.B., Daughney, C.J., Yee, N., Davis, T.A., 1997. A chemical equilibrium model for metal adsorption onto bacterial surfaces. *Geochimica et Cosmochimica Acta* 61, 3319–3328.
- Flaathen, T.K., Gislason, S.R., Oelkers, E.H., 2010. The effect of aqueous sulphate on basaltic glass dissolution rates. *Chemical Geology* 277, 345–354.
- Ganor, J., Reznik, I.J., Rosenberg, Y.O., 2009. Organics in water–rock interactions. *Reviews in Mineralogy and Geochemistry* 70, 259–369.
- Gislason, S.R., Oelkers, E.H., 2003. Mechanism, rates and consequences of basaltic glass dissolution: II. An experimental study of the dissolution rates of basaltic glass as a function of pH and temperature. *Geochimica et Cosmochimica Acta* 67, 3817–3832.
- Gislason, S.R., Wolff-Boenisch, D., Stefansson, A., Oelkers, E.H., Gunnlaugsson, E., Sigurdardóttir, H., Sigfússon, G., Brocker, W.S., Matter, J., Stute, M., Axelsson, G., Fridriksson, T., 2010. Mineral sequestration of carbon dioxide in basalt: a pre-injection overview of the CarbFix project. *International Journal of Greenhouse Gas Control* 4, 537–545.
- Gout, R., Oelkers, E.H., Schott, J., Zwick, A., 1997. The surface chemistry and structure of acid-leached albite: new insights on the dissolution mechanism of the alkali feldspars. *Geochimica et Cosmochimica Acta* 61, 3013–3018.
- Grantham, M.C., Dove, P.M., Dichristina, T.J., 1997. Microbially catalyzed dissolution of iron and aluminum oxyhydroxide mineral surface coatings. *Geochimica et Cosmochimica Acta* 61, 4467–4477.
- Hopf, J., Langenhorst, F., Pollok, K., Mertean, D., Kothe, E., 2009. Influence of microorganisms on biotite dissolution: an experimental approach. *Chemie der Erde* 69, 45–56.
- Hutchens, E., 2009. Microbial selectivity on mineral surfaces: possible implications for weathering processes. *Fungal Biology Reviews* 23, 115–121.
- Hutchens, E., Valsami-Jones, E., McEldowney, S., Gaze, W., McLean, J., 2003. The role of heterotrophic bacteria in feldspar dissolution – an experimental approach. *Mining Magazine* 67, 1157–1170.
- Hutchens, E., Valsami-Jones, E., Harouiya, N., Chairat, C., Oelkers, E.H., McEldowney, S., 2006. An experimental investigation of the effect of *Bacillus megaterium* on apatite dissolution. *Geomicrobiology Journal* 23, 177–182.
- Hutchens, E., Gleeson, D., McDermott, F., Miranda-Casoluengo, R., Clipson, N., 2010. Meter-scale diversity of microbial communities on a weathered pegmatite granite outcrop in the Wicklow Mountains, Ireland; evidence for mineral induced selection? *Geomicrobiology Journal* 27, 1–14.
- Johnson, K.J., Ams, D.A., Wedel, A.N., Szymanowski, J.E.S., Weber, D.L., Schneegurt, M.A., Fein, J.B., 2007. The impact of metabolic state on Cd adsorption onto bacterial cells. *Geobiology* 5, 211–218.
- Kalinowski, B.E., Liermann, L.J., Givens, S., Brantley, S.L., 2000. Rates of bacteria-promoted solubilization of Fe from minerals: a review of problems and approaches. *Chemical Geology* 169, 357–370.
- Kenward, P.A., Goldstein, G.H., González, L.A., Roberts, J.A., 2009. Precipitation of low-temperature dolomite from an anaerobic microbial consortium: the role of methanogenic Archaea. *Geobiology* 7, 556–565.
- Knauer, K., Behra, R., Sigg, L., 1997. Effects of free Cu²⁺ and Zn²⁺ ions on growth and metal accumulation in freshwater algae. *Environmental Toxicology and Chemistry* 16, 220–229.
- Koroleff, F., 1976. Determination of silicon. In: Grasshoff, K. (Ed.), *Methods of Seawater Analysis*. Springer Verlag, New York, pp. 149–158.
- Le Faucher, S., Behra, R., Sigg, L., 2005. Thiol and metal contents in periphyton exposed to elevated copper and zinc concentrations: a field and microcosm study. *Environmental Science and Technology* 36, 8099–8107.
- Lee, J.-U., Fein, J.B., 2000. Experimental study of the effects of *Bacillus subtilis* on gibbsite dissolution rates under near-neutral pH and nutrient-poor conditions. *Chemical Geology* 166, 193–202.
- Liermann, L.J., Kalinowski, B.E., Brantley, S.L., Ferry, J.G., 2000a. Role of bacterial siderophores in dissolution of hornblende. *Geochimica et Cosmochimica Acta* 64, 587–602.
- Liermann, L.J., Barnes, A.S., Kalinowski, B.E., Zhao, X., Brantley, S.L., 2000b. Microenvironments of pH in biofilms grown on dissolving silicate surfaces. *Chemical Geology* 171, 1–16.
- Lüttge, A., Conrad, P.G., 2004. Direct observation of microbial inhibition of calcite dissolution. *Applied and Environmental Microbiology* 70, 1627–1632.
- Malinowskaya, I.M., Kosenko, L.V., Votselko, S.K., Podgorskii, V.S., 1990. Role of *Bacillus mucilaginosus* polysaccharide in degradation of silicate minerals. *Mikrobiologiya* 59, 70–78 (Engl. Transl. p. 49–55).
- Martinez, R.E., Pokrovsky, O.S., Schott, J., Oelkers, E.H., 2008. Surface charge and zeta-potential of metabolically active and dead cyanobacteria. *Journal of Colloid and Interface Science* 323, 317–325.
- Martinez, R.E., Gardés, E., Pokrovsky, O.S., Schott, J., Oelkers, E.H., 2010. Do photosynthetic bacteria have a protective mechanism against carbonate precipitation at their surfaces? *Geochimica et Cosmochimica Acta* 74, 1329–1337.
- Maurice, P.A., Vierkorn, M.A., Hersman, L.E., Fulghum, J.E., Ferryman, A., 2001. Enhancement of kaolinite dissolution by an aerobic *Pseudomonas mendocina* bacterium. *Geomicrobiology Journal* 18, 21–35.
- Nazina, T.N., Luk'yanova, E.A., Zakharova, E.V., Ivoilov, V.S., Poltarau, A.B., Kalmykov, S.N., Belyaev, S.S., Zubkov, A.A., 2006. Distribution and activity of microorganisms in the deep repository for liquid radioactive waste at the Siberian chemical combine. *Microbiology* 75, 727–738.
- Nazina, T.N., Luk'yanova, E.A., Zakharova, E.V., Konstantinova, L.L., Kalmykov, S.N., Poltarau, A.B., Zubkov, A.A., 2010. Microorganisms in a disposal site for liquid radioactive wastes and their influence on radionuclides. *Geomicrobiology Journal* 27, 473–486.
- Neaman, A., Chorover, J., Brantley, S.L., 2005a. Implications of the evolution of organic acid moieties for basalt weathering over geological time. *American Journal of Science* 305, 147–185.
- Neaman, A., Chorover, J., Brantley, S.L., 2005b. Element mobility patterns records organics ligands in soils on early Earth. *Geology* 33, 117–120.
- Neaman, A., Chorover, J., Brantley, S.L., 2006. Effects of organic ligands on granite dissolution in batch experiments at pH 6. *American Journal of Science* 306, 451–473.
- Ngwenya, B.T., 2007. Enhanced adsorption of zinc is associated with aging and lysis of bacterial cells in batch incubations. *Chemosphere* 67, 1982–1992.
- Oelkers, E.H., 2001. General kinetic description of multioxide silicate mineral and glass dissolution. *Geochimica et Cosmochimica Acta* 65, 3703–3719.
- Oelkers, E.H., Gislason, S.R., 2001. The mechanism, rates and consequences of basaltic glass dissolution: I. An experimental study of the dissolution rates of basaltic glass as a function of aqueous Al, Si and oxalic acid concentration at 25 °C and pH = 3 and 11. *Geochimica et Cosmochimica Acta* 65, 3671–3681.
- Oelkers, E.H., Schott, J., 1998. Does organic acid adsorption affect alkali-feldspar dissolution rates? *Chemical Geology* 155, 235–245.
- Oelkers, E.H., Schott, J., 2005. Geochemical aspects of CO₂ sequestration. *Chemical Geology* 217, 183–186.
- Oelkers, E.H., Gislason, S.R., Matter, J., 2008a. Mineral carbonation of CO₂. *Elements* 4, 333–337.
- Oelkers, E.H., Schott, J., Gauthier, J.-M., Herrero-Roncal, T., 2008b. An experimental study of the dissolution rates of muscovite. *Geochimica et Cosmochimica Acta* 72, 4948–4961.
- Parkhurst, D.L., Appelo, C.A.J., 1999. User's guide to PHREEQC (version 2) – a computer program for speciation, batch-reaction, one-dimensional transport, and inverse geochemical calculations. Washington, DC: U.S. Geological Survey Water-Resources Investigations Report 99–4259. 312 pp.
- Pedersen, K., 1997. Microbial life in deep granitic rock. *FEMS Microbiology Reviews* 20, 399–414.
- Pedros-Alíó, C., 2006. Marine microbial diversity: can it be determined? *Trends in Microbiology* 14, 257–263.
- Pokrovsky, O.S., Martinez, R.E., Golubev, S.V., Kompantseva, E.I., Shirokova, L.S., 2008. Adsorption of metals and protons on *Gloeocapsa* sp. cyanobacteria: a surface speciation approach. *Applied Geochemistry* 23, 2574–2588.
- Pokrovsky, O.S., Shirokova, L.S., Bénéžeth, P., Schott, J., Golubev, S.V., 2009. Effect of organic ligands and heterotrophic bacteria on wollastonite dissolution kinetics. *American Journal of Science* 309, 731–772.
- Pokrovsky, O.S., Shirokova, L.S., Bénéžeth, P., Schott, J., Golubev, S.V., 2010. Reply to Comment by R. A. Berner on “Effect of organic ligands and heterotrophic bacteria on Wollastonite dissolution kinetics”. *American Journal of Science* 309, 731–772.
- Am. J. Sci. 310, 425–426.
- Robert, M., Berthelin, J., 1986. Role of biological and biochemical factors in soil mineral weathering. In: Huang, P.M., Schnitzer, M. (Eds.), *Interactions of Soil Minerals with Natural Organics and Microbes*. Soil Science Society of America, Madison, Wisconsin, pp. 453–495.
- Rogers, J.R., Bennett, P.C., 2004. Mineral stimulation of subsurface microorganisms: release of limiting nutrients from silicates. *Chemical Geology* 203, 91–108.
- Santelli, C., Welch, S.A., Westrich, H.R., Banfield, J.F., 2001. The effect of Fe-oxidizing bacteria on Fe-silicate mineral dissolution. *Chemical Geology* 180, 99–115.
- Schott, J., Pokrovsky, O.S., Oelkers, E.H., 2009. The link between mineral dissolution/precipitation kinetics and solution chemistry. *Reviews in Mineralogy and Geochemistry* 70, 207–258.
- Shirokova, L.S., Bénéžeth, P., Pokrovsky, O.S., 2009. Effect of heterotrophic bacteria extracted from groundwater on Ca silicate dissolution. *Geochimica et Cosmochimica Acta* 73, A1213.
- Shirokova, L.S., Bénéžeth, P., Pokrovsky, O.S., Gérard, E., Ménez, B., Alfredsson, H., 2012. Effect of the heterotrophic bacterium *Pseudomonas reactans* on olivine dissolution kinetics and implications for CO₂ storage in basalts. *Geochimica et Cosmochimica Acta* 80, 30–50. doi:10.1016/j.gca.2011.11.046.
- Sinclair, J.L., Ghiorse, W.C., 1989. Distribution of aerobic bacteria, protozoa, algae, and fungi in deep subsurface sediments. *Geomicrobiology Journal* 7, 15–31.
- Stevens, T.O., McKinley, J.P., 1995. Lithoautotrophic microbial ecosystems in deep basalt aquifers. *Science* 270, 450–454.
- Stockmann, G.J., Wolff-Boenisch, D., Gislason, S.R., Oelkers, E.H., 2011. Do carbonate precipitates affect dissolution kinetics? 1: Basaltic glass. *Chemical Geology* 284, 306–316.
- Sverdrup, H., 2009. Chemical weathering of soil minerals and the role of biological processes. *Fungal Biology Reviews* 23, 94–100.
- Thorseth, I.H., Furnes, H., Heldal, M., 1992. The importance of microbiological activity in the alteration of natural basaltic glass. *Geochimica et Cosmochimica Acta* 56, 845–850.
- Thorseth, I.H., Furnes, H., Tumor, O., 1995. Textural and chemical effects of bacterial activity on basaltic glass: an experimental approach. *Chemical Geology* 119, 139–160.
- Ullman, W.J., Kirchman, D.L., Welch, S.A., Vandevivere, P., 1996. Laboratory evidence for microbially mediated silicate mineral dissolution in nature. *Chemical Geology* 132, 11–17.
- Uroz, S., Calvaruso, Ch., Turpault, M.-P., Frey-Klett, P., 2009. Mineral weathering by bacteria: ecology, actors and mechanisms. *Trends in Microbiology* 17, 378–387.

- Urrutia Mera, M., Kemper, M., Doyle, R., Beveridge, T.J., 1992. The membrane-induced proton motive force influences the metal binding ability of *Bacillus subtilis* cell walls. *Applied and Environmental Microbiology* 58, 3837–3844.
- Valsami-Jones, E., McEldowney, S., 2000. Mineral dissolution by heterotrophic bacteria: principles and methodologies. *Environmental Mineralogy: Microbial Interactions, Anthropogenic Influences, Contaminated Land and Waste Management*. Mineralogical Society Series, London, U.K., pp. 27–55.
- Vandevivere, P., Welch, S.A., Ullman, W.J., Kirchman, D.L., 1994. Enhanced dissolution of silicate minerals by bacteria at near-neutral pH. *Microbial Ecology* 27, 241–251.
- Webley, D.M., Duff, R.B., Mitchell, W.A., 1960. Plate method for studying the breakdown of synthetic and natural silicates by soil bacteria. *Nature* 188, 766–767.
- Webley, D.M., Henderson, M.E.K., Taylor, I.F., 1963. The microbiology of rocks and weathered stones. *Journal of Soil Science* 14, 102–112.
- Welch, S.A., Banfield, J.F., 2002. Modification of olivine surface morphology and reactivity by microbial activity during chemical weathering. *Geochimica et Cosmochimica Acta* 66, 213–221.
- Welch, S.A., Ullman, W.J., 1993. The effect of organic acids on plagioclase dissolution rates and stoichiometry. *Geochimica et Cosmochimica Acta* 57, 2725–2736.
- Welch, S.A., Vandevivere, P., 1994. Effect of microbial and other naturally occurring polymers on mineral dissolution. *Geomicrobiology Journal* 12, 227–238.
- Welch, S.A., Barker, W.W., Banfield, J.F., 1999. Microbial extracellular polysaccharides and plagioclase dissolution. *Geochimica et Cosmochimica Acta* 63, 1405–1419.
- Wolff-Boenisch, D., Gislason, S.R., Oelkers, E.H., 2004a. The effect of fluoride on the dissolution rates of natural glasses at pH 4 and 25 °C. *Geochimica et Cosmochimica Acta* 68, 4571–4582.
- Wolff-Boenisch, D., Gislason, S.R., Oelkers, E.H., Putnis, C.V., 2004b. The dissolution rates of natural glasses as a function of their composition at pH 4 and 10.6, and temperatures from 25 to 74 °C. *Geochimica et Cosmochimica Acta* 68, 4843–4858.
- Wolff-Boenisch, D., Gislason, S.R., Oelkers, E.H., 2006. The effect of crystallinity on dissolution rates and CO₂ consumption capacity of silicates. *Geochimica et Cosmochimica Acta* 70, 858–870.
- Wolff-Boenisch, D., Wenau, S., Gislason, S.R., Oelkers, E.H., 2011. Dissolution of basalts and peridotite in seawater, in the presence of ligands, and CO₂: implications for mineral sequestration of carbon dioxide. *Geochimica et Cosmochimica Acta* 75, 5510–5525.
- Wu, L., Jacobson, A.D., Chen, H.-C., Hausner, M., 2007. Characterization of elemental release during microbe–basalt interactions at T = 28 °C. *Geochimica et Cosmochimica Acta* 71, 2224–2239.
- Wu, L., Jacobson, A.D., Hausner, M., 2008. Characterization of elemental release during microbe–granite interactions at T = 28 °C. *Geochimica et Cosmochimica Acta* 72, 1076–1095.
- Yeghicheyan, D., Carignan, J., Valladon, M., Le Coz, M.B., Cornec, F.L., Castrec-Rouelle, M., Robert, M., Aquilina, L., Aubry, E., Churlaud, C., Dia, A., Deberdt, S., Dupré, B., Freydier, R., Gruau, G., Hénin, O., de Kersabiec, A.-M., Macé, J., Marin, L., Morin, N., Petitjean, P., Serrat, E., 2001. A compilation of silicon and thirty one trace elements measured in the natural river water reference material SLRS-4 (NRC-CNRC). *Geostandards Newsletter* 25, 465–474.